The draining lymph nodes (inguinal and axillary) were removed from the mice at the indicated time intervals for flow cytometric analysis and cytotoxicity assay.

Immunohistochemical analysis

Rabbit anti-mouse CCR5 polyclonal antibodies were prepared as described previously [25]. The removed tumor tissues were embedded in paraffin or the Sakura Tissue-Tek OCT compound (Sakura Finetek, Torrance, CA, USA) as frozen tissues. The paraffin-embedded sections were then stained with goat anti-mouse CCR1 (Santa Cruz Biotechnology, Santa Cruz, CA, USA), rabbit anti-CCR5, goat anti-mouse CCL3 (R&D Systems, Minneapolis, MN, USA), rat anti-mouse F4/80, anti-mouse CD3 (Serotec, Oxford, UK), rabbit anti-ssDNA, or rat anti-Ki67 (Dako Cytomation, Tokyo, Japan) overnight at 4°C. Cryostat sections of the frozen tissues were fixed with 4% paraformaldehyde (PFA) in PBS and stained with rat anti-mouse DEC205 (Serotec) or hamster anti-mouse CD11c (BD Biosciences) overnight at 4°C. The sections were then incubated for 1 h at room temperature with biotinylated rabbit anti-goat IgG, biotinylated swine anti-rabbit IgG, biotinylated rabbit anti-rat IgG (Dako Cytomation), or biotinylated mouse anti-hamster IgG (BD Biosciences). The immune complexes were visualized using a catalyzed signal amplification system (Dako Cytomation) or the ELITE avidin-biotin-peroxidase and diaminobenzidine substrate kits (Vector Laboratories, Burlingame, CA, USA), except for anti-ssDNA, where a novel HRP-labeled polymer (Envision$^+$, Dako Cytomation) was used, according to the manufacturer's instructions. As a negative control, goat IgG (R&D Systems), rabbit IgG (Dako Cytomation), rat IgG (Cosmo Bio, Tokyo, Japan), or hamster IgG (BD Biosciences) was used instead of specific primary antibodies. The numbers of positive cells were determined in each animal in 10 randomly chosen fields at 400-fold magnification by an examiner without any prior knowledge of the experimental procedures.

Double-color immunofluorescence analysis

Tumor tissues were embedded in paraffin or the OCT compound as frozen tissues. The paraffin-embedded sections were then stained with combinations of rat anti-mouse CD3 and goat anti-mouse CCL3 or anti-F4/80 and anti-CCL3 antibodies overnight at 4°C. After fixation with 4% PFA/PBS, cryostat sections were stained with the combinations rat anti-mouse CD4 (BD Biosciences) and anti-CCR1, rat anti-mouse CD8a (BD Biosciences) and anti-CCR1, anti-CD4 and anti-CCR5, anti-CD8a and anti-CCR5, rat anti-DEC205 and anti-CCR1, anti-DEC205 and anti-CCR5, PE-conjugated hamster anti-CD11c (BD Biosciences) and anti-CCR1, PE-conjugated anti-CD11c and anti-CCR5, PE-conjugated anti-CD11c and rat anti-CD11b (BD Biosciences), or PE-conjugated anti-CD11c and anti CD8a antibodies. After extensive washing, AF488 donkey anti-rat IgG (Invitrogen, Carlsbad, CA, USA) was applied as the secondary antibody to detect CD4-, CD8a-, CD3-, F4/80-, DEC205-, or CD11b-positive cells. Simultaneously, AF546 or AF488 donkey anti-goat IgG (Invitrogen) was used to detect CCR1- or CCL3-positive cells, and AF594 or AF488 donkey anti-rabbit IgG (Invitrogen) was used to detect CCR5-positive cells. The sections were observed using a confocal microscope (LSM 510 META, Zeiss, Thornwood, NY, USA). The percentage of double-positive cells was determined in each animal in five randomly chosen fields at 400-fold magnification by an examiner without any prior knowledge of the experimental procedures.

Flow cytometric analysis

Inguinal and axillary lymph nodes were removed and digested in a DNase I and collagenase solution (Sigma Chemical Co.). The resultant, single-cell preparations were stained with various combinations of FITC-labeled anti-CD4, FITC-labeled anti-CD86, PE-labeled anti-CD8, PE-labeled anti-CD11c, PE-labeled anti-CD44, and PE-labeled anti-CD62 ligand (CD62L) mAb (BD Biosciences). FITC-rat IgG, PE-hamster IgG, and PE-rat IgG were used as isotype controls (BD Biosciences). To prepare the tumor lysate, BNL or CT26 cells were suspended in PBS and subjected to four cycles of rapid freezing in liquid nitrogen and thawing at 55°C. The lysate was spun at 15,000 rpm to remove particulate cellular debris. To stain intracellular IFN-γ, the mononuclear cells harvested from the draining lymph nodes on Day 8 (see Fig. 5A) were incubated with the BNL or CT26 lysates at a tumor cell:mononuclear cell ratio of 1:1 in the presence of GolgiPlug (BD Biosciences). Six hours later, surface staining was performed with APC-conjugated CD8 antibodies. Intracellular IFN-γ was stained after fixation and permeabilization with BD Cytofix/Cytoperm buffer with PE-conjugated IFN-γ antibodies or isotype control using the Mouse Intracellular Cytokine Staining starter kit (BD Biosciences). At least 100,000 stained cells were analyzed on a FACSCalibur system for each determination. The data were expressed as a proportion of positive cells (compared with cells stained with an irrelevant control antibody), and the absolute positive cell numbers were calculated after determining the total cell numbers in the lymph nodes by the following formula: Absolute positive cell numbers = total cell number in the lymph nodes × percentage of positive cells × 1/100.

Quantitative real-time RT-PCR

Total RNA was extracted from the resected tumor and lymph nodes using RNA-Bee (Tel-Test, Friendswoods, TX, USA), according to the manufacturer's instructions. After the RNA preparations were further treated with RNase-free DNase I (Life Technologies, Gaithersburg, MD, USA) to remove residual DNA, cDNA was synthesized as described previously [26]. Quantitative real-time PCR was performed on an Applied Biosystems StepOne™ real-time PCR system (Applied Biosystems, Foster City, CA, USA) using the comparative threshold (C_T) quantification method. TaqMan® gene expression assays (Applied Biosystems) containing specific primers (Accession Numbers CCL3, Mm00441258_ml; CCL4, Mm00443111_m1; CCL5, Mm01302428_ml; CCR1, Mm00438260_s1; CCR5, Mm01216171_m1; GAPDH, Mm99999915_g1), TaqMan® minor groove binder probe (FAM™ dye-labeled), and TaqMan® fast universal PCR master mix were used with 10 ng cDNA to detect and quantify the expression levels of CCL3, CCL4, CCL5, CCR1, and CCR5. Reactions were performed for 20 s at 95°C and then for 40 cycles of 1 s at 95°C and 20 s at 60°C. GAPDH was amplified as an internal control. C_T values of GAPDH were subtracted from C_T values of the target genes (ΔC_T). ΔC_T values of tumors after GCV injection were compared with ΔC_T values of tumors before GCV injection.

Cytotoxicity assay

Mononuclear cells were isolated from the draining lymph nodes at the indicated time intervals and were incubated at a cell density of 2×10^6 cells/ml in the presence of 0.6×10^6 cells/ml BNL cells, which were irradiated at 50 Gy beforehand. After 5 days of culture, the cells were tested for cytotoxicity in a lactate dehydrogenase assay using the CytoTox 96 nonradioactive cytotoxicity assay kit (Promega, Madison, WI, USA), according to the manufacturer's instructions. Effector cells were added to target cells in triplicate at different E:T ratios. Percentage of specific lysis was calculated using the following formula: [(experimental−effector spontaneous−target spontaneous)/(target maximum−target spontaneous)] × 100%.

Adoptive transfer of DC

Draining lymph nodes were harvested on Day 8 (see Fig. 5A) and were digested with DNase I and collagenase solution. Mononuclear cells were obtained by centrifugation over a Histopaque-1077 density gradient (Sigma Chemical Co.), and DCs were isolated by CD11c-conjugated magnetic microbeads (Miltenyi Biotec, Auburn, CA, USA). CD11c-positive DCs (2.5×10^5/mouse) were injected into the left flank of GCV-treated KO mice on Day 8 (see Fig. 5A). On Day 18, DC-transferred mice were rechallenged with 1×10^5 BNL cells in their right flank, and tumor sizes were measured.

Statistical analysis

Data were analyzed statistically using one-way ANOVA followed by the Tukey-Kramer test, except for tumor progression data, which were analyzed using two-way ANOVA. Data of tumor sizes after adoptive transfer of the DC experiment were analyzed using the Mann-Whitney U test. $P < 0.05$ was considered statistically significant.

RESULTS

GCV treatment induces tumor cell apoptosis with intratumoral CCR1-, CCR5-, and CCL3-positive cell accumulation in WT mice

We investigated whether HSV-tk-GCV treatment can induce apoptosis in vitro in the tk-transfected murine hepatoma cell line BNL-tk. GCV treatment significantly increased the proportions of early (annexin-positive but PI-negative) and late (annexin-positive and PI-positive) apoptotic cells (Fig. 1, A and B). We injected GCV into WT mice i.p. after the s.c. BNL-tk tumor was formed macroscopically, according to the schedule, as shown in Figure 1C. Microscopic analysis revealed that more than half of the tumor cells were apoptotic and that a large number of mononuclear cells had accumulated in the tumor sites on Day 19 immediately following the completion of treatment (Fig. 1D and Supplemental Fig. 1). Thereafter, the tumor regressed macroscopically. We next investigated the chemokine receptor expression by tumor-infiltrating cells after the induction of in vivo tumor apoptosis by suicide gene therapy. Immunohistochemical analysis revealed the presence of few CCR1-, CCR5-, or CCL3-positive cells in tumors without GCV treatment (**Fig. 2A**). In contrast, GCV treatment caused intratumoral infiltration of a large number of CCR1-, CCR5-, and CCL3-positive cells in WT mice, along with massive apoptosis of tumor cells (Fig. 2A and Supplemental Fig. 2). The intratumoral mRNA expression of CCL3, CCL4, and CCL5 was markedly increased 3 days after GCV treatment, whereas that of their receptors CCR1 and CCR5 was augmented later than 3 days after GCV injection (Fig. 2B).

Tumor-infiltrating DCs express CCR1 and CCR5

To determine the type of tumor-infiltrating cells expressing CCR1, CCR5, or CCL3, we performed a double-color immunofluorescence analysis. CD4- and CD8-positive T cells expressed CCR5 but not CCR1 (**Fig. 3A** and Supplemental Fig. 3A; 78.2±8.9% of CD4-positive T cells and 92.6±8.2% of CD8-positive T cells expressed CCR5, and CCR1 was not detected in CD4- or CD8-positive T cells). In contrast, CD11c- and DEC205-positive cells, which infiltrated to tumor sites of WT mice after GCV treatment, expressed CCR1 and CCR5 (Fig. 3B and Supplemental Fig. 3B; 100% of CD11c-positive DCs expressed CCR1 and CCR5, 97.5±5.6% DEC205-positive cells expressed CCR1, and 100% DEC-positive cells expressed CCR5). Moreover, tumor-infiltrating, CD11c-positive DCs exhibited a "myeloid" phenotype, as 87.8 ± 14.8% of CD11c-positive cells expressed CD11b, and none of them expressed CD8a (Supplemental Fig. 3C). Furthermore, CCL3 proteins were detected in CD3-positive T cells, F4/80-positive macrophages (Fig. 3C; 72.0±9.1% of CD3-positive T cells and 87.0±12.0% of F4/80-positive macrophages expressed CCL3). These observations suggest that apoptosis induced by GCV treatment enhanced the expression of CCL3, CCL4, and CCL5 and then produced chemokines attracted to CD11c-positive DCs as well as CD3-positive T cells. To address this possibility, we investigated intratumoral infiltration of CD11c-positive DCs and CD3-positive T cells in CCR1KO, CCR5KO, or CCL3KO mice, which were s.c.-inoculated with 2×10^5 BNL-tk cells into WT and KO mice. The lack of CCR1, CCR5, or CCL3 had no discernible effects on the growth of primary tumors (**Fig. 4A**). Then, we injected GCV i.p. into the mice as shown in Figure 1C. Immunohistochemical analysis revealed

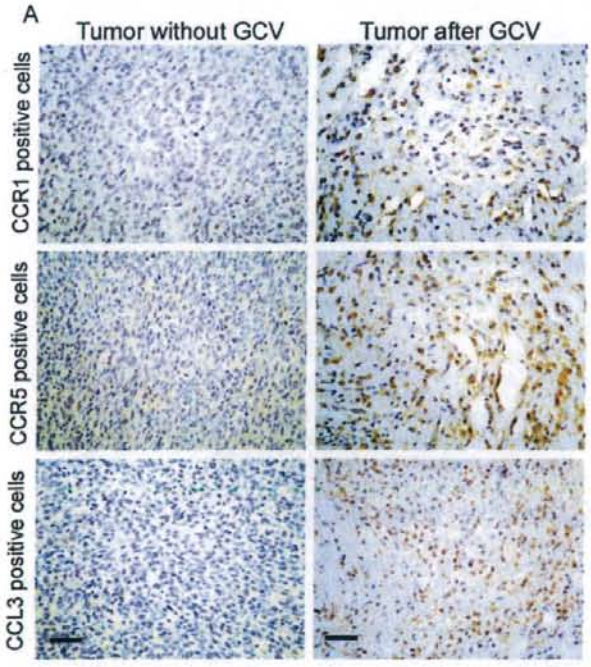

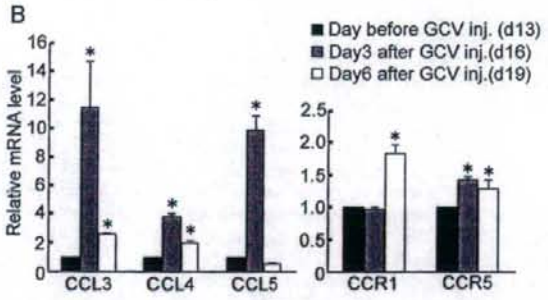

Fig. 2. Accumulation of tumor-infiltrating CCR1-, CCR5-, or CCL3-positive cells after tumor apoptosis induced by GCV treatment. Mice were inoculated with BNL-tk cells according to the schedule shown in Figure 1C. (A) Tumors were removed from WT mice on Day 19, and immunohistochemical analysis was performed using anti-CCR1, -CCR5, or -CCL3 antibody on tumors with or without GCV treatment. Representative results from three individual animals in each group are shown here. Original magnification, ×400. Original bars, 50 μm. (B) Real-time RT-PCR was performed on total RNA extracted from the tumor of WT mice harvested on Days 13, 16, or 19. The level of chemokine mRNA was normalized to GAPDH mRNA levels. Bars, ±1 SD (n=3); *, $P < 0.05$, compared with the day before GCV injection.

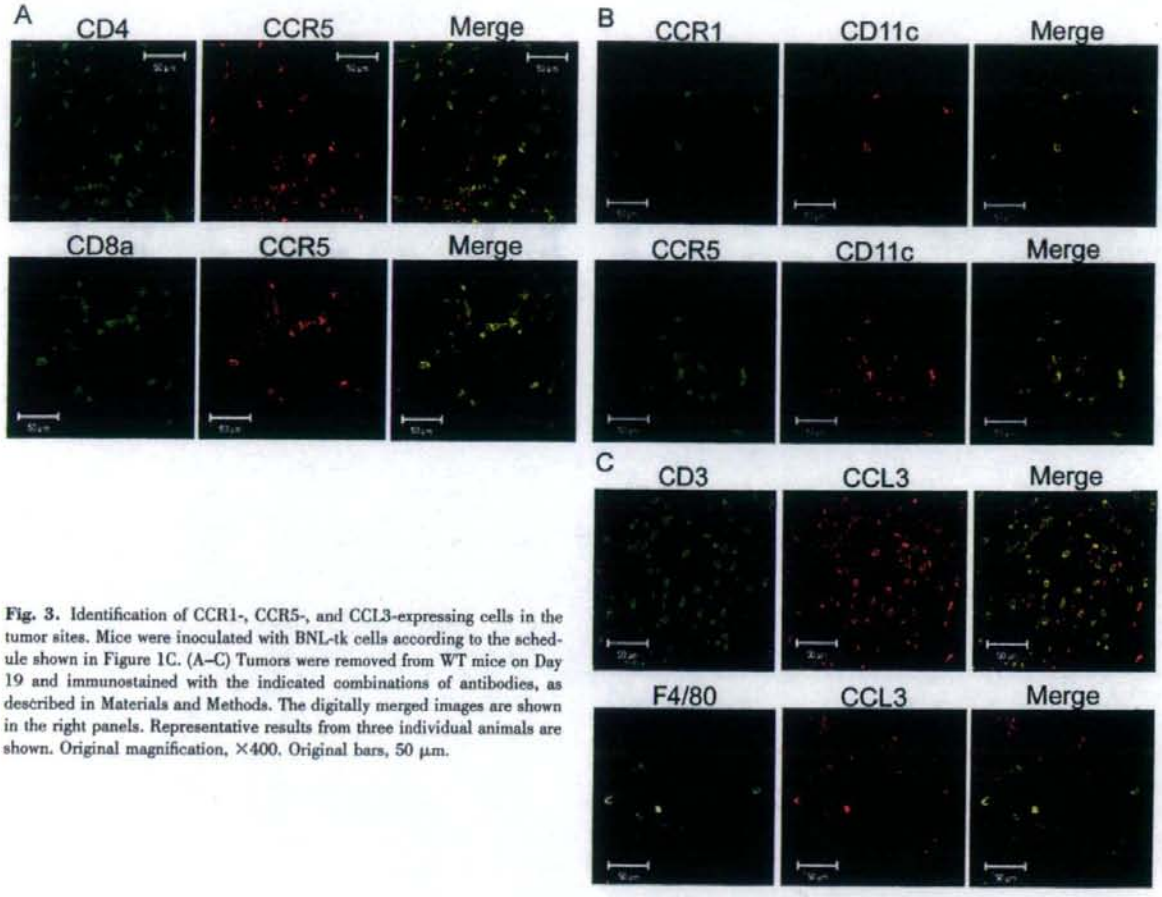

Fig. 3. Identification of CCR1-, CCR5-, and CCL3-expressing cells in the tumor sites. Mice were inoculated with BNL-tk cells according to the schedule shown in Figure 1C. (A–C) Tumors were removed from WT mice on Day 19 and immunostained with the indicated combinations of antibodies, as described in Materials and Methods. The digitally merged images are shown in the right panels. Representative results from three individual animals are shown. Original magnification, ×400. Original bars, 50 μm.

the presence of few CD3-, F4/80-, or DEC205-positive cells in tumors without GCV treatment (Fig. 4B). GCV treatment induced tumor cell apoptosis in CCL3KO, CCR1KO, and CCR5KO mice to a similar extent as that in WT mice (data not shown). Moreover, GCV treatment caused intratumoral accumulation of a large number of CD3-, CD4-, and CD8-positive T cells and DEC205- and CD11c-positive DCs in WT mice (Fig. 4, B and C). By contrast, the increases in intratumorally accumulating DEC205- and CD11c-positive cells and to a lesser extent, CD3-, CD4-, and CD8-positive cells were attenuated in CCR1KO, CCR5KO, and CCL3KO mice (Fig. 4, B and C). In contrast, GCV treatment induced intratumoral infiltration of F4/80-positive macrophages (Fig. 4B) and CD49b/DX5-positive NK cells (data not shown) in WT and KO mice to a similar extent.

Partial failure of CCR1KO, CCR5KO, and CCL3KO mice in rejecting the rechallenged tumor

Apoptosis induced by GCV treatment caused intratumoral infiltration of DCs and T cells in a CCR1- and/or CCR5-dependent manner. As intratumoral infiltration of DCs and T cells is a prerequisite for the establishment of specific tumor immunity, we examined the immune status of GCV-treated mice by rechallenging the parental BNL cell line. To completely eradicate the primary BNL-tk tumor, GCV was administered between 2 and 5 days after the tumor injection (**Fig. 5A**). Primary BNL-tk tumors were eradicated completely in WT, CCR1KO, CCR5KO, and CCL3KO mice at similar rates (data not shown). When these mice were injected again with parental BNL cells, WT mice rejected them completely. In contrast, CCR1KO, CCR5KO, and CCL3KO mice failed to completely eliminate the rechallenged tumor cells, although the growth rates were retarded in these mice compared with naïve WT mice (Fig. 5B). A marked cytotoxicity against BNL but not in CT26 cells was observed when draining lymph node-derived mononuclear cells of GCV-treated WT mice were used as effector cells. Only a modest amount of cytotoxicity was detected when mononuclear cells in the draining lymph nodes of GCV-treated CCR1KO, CCR5KO, or CCL3KO mice were used as effector cells (Fig. 5C). Further, GCV-induced tumor apoptosis enhanced the mRNA expression of Th1 cytokines such as IFN-γ, IL-12p40, and IL-18 in the draining lymph nodes of WT mice but not of CCR1KO, CCR5KO, and CCL3KO mice (Supplemental Fig. 4). Likewise, $CD8^+IFN\text{-}\gamma^+$ cells were increased markedly in GCV-treated WT mice when lymph node-derived mononuclear cells were cocultured with BNL cell lysates, compared with tumor-bearing or tumor-free

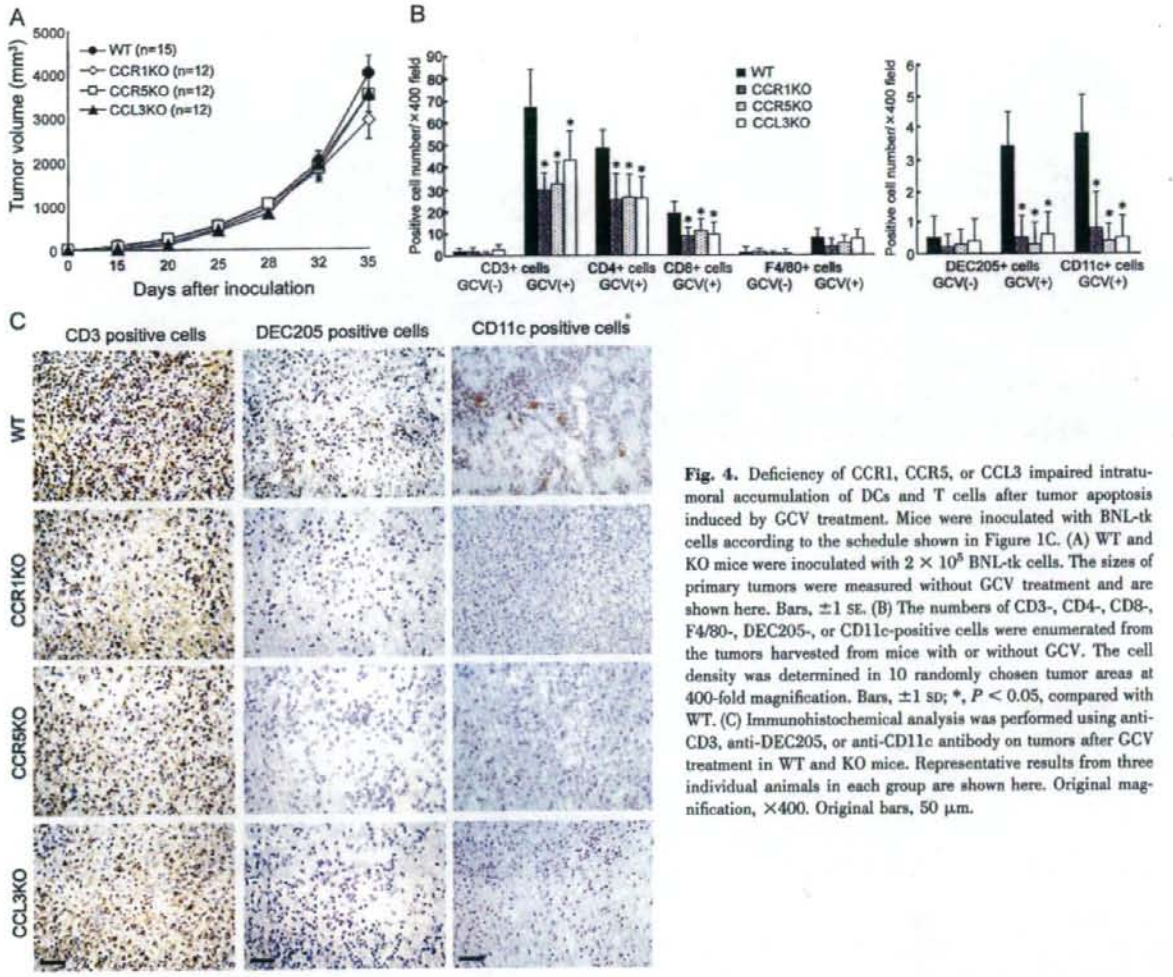

Fig. 4. Deficiency of CCR1, CCR5, or CCL3 impaired intratumoral accumulation of DCs and T cells after tumor apoptosis induced by GCV treatment. Mice were inoculated with BNL-tk cells according to the schedule shown in Figure 1C. (A) WT and KO mice were inoculated with 2×10^5 BNL-tk cells. The sizes of primary tumors were measured without GCV treatment and are shown here. Bars, ±1 SE. (B) The numbers of CD3-, CD4-, CD8-, F4/80-, DEC205-, or CD11c-positive cells were enumerated from the tumors harvested from mice with or without GCV. The cell density was determined in 10 randomly chosen tumor areas at 400-fold magnification. Bars, ±1 SD; *, $P < 0.05$, compared with WT. (C) Immunohistochemical analysis was performed using anti-CD3, anti-DEC205, or anti-CD11c antibody on tumors after GCV treatment in WT and KO mice. Representative results from three individual animals in each group are shown here. Original magnification, ×400. Original bars, 50 μm.

WT mice (Fig. 5D). Increases in $CD8^+IFN\text{-}\gamma^+$ cells were less evident in CCR1KO, CCR5KO, or CCL3KO mice treated with tumor cells and GCV compared with WT mice when lymph node-derived cells were cocultured with BNL cell lysates (Fig. 5D). These observations suggest that the absence of CCR1, CCR5, or CCL3 greatly impaired the apoptosis-induced establishment of specific tumor immunity.

Apoptosis-induced migration of DCs to draining lymph nodes and intranodal T cell proliferation activation in a CCR1-, CCR5-, and/or CCL3-dependent manner

Tumor-infiltrating DCs can uptake tumor antigens at the tumor sites and migrate to the draining lymph nodes, where they mature to present antigens to T cells [17, 18]. Thus, we further explored the status of DCs as well as T cells in the draining lymph nodes. Following GCV treatment, tumor apoptosis increased the proportions of $CD86^+CD11c^+$ cells in the draining lymph nodes but not in distant lymph nodes in WT mice (**Fig. 6A**). In contrast, GCV-induced increases in $CD11c^+$ cell proportion were depressed in CCR1KO, CCR5KO, or CCL3KO mice (Fig. 6A). The levels of CD86 on $CD11c^+$ cells were increased in GCV-treated WT mice compared with WT mice, which had been injected with neither BNL-tk cells nor GCV, although the levels of CD86 were depressed in the KO mice (mean fluorescent intensities of CD86 on $CD11c^+$ cells: WT/BNL-tk/GCV, 114.3±8.6; WT/BNL-tk, 86.2±12.2; WT/no tumor, 86.5±2.6; CCR1KO/BNL-tk/GCV, 85.4±15.6; CCR5KO/BNL-tk/GCV, 92.3±12.6; CCL3KO/BNL-tk/GCV, 79.0±9.8). Moreover, GCV-induced tumor apoptosis significantly increased the numbers of total cells, $CD4^+$ and $CD8^+$ cells, in the draining lymph nodes of WT mice. GCV-induced increases in these cell populations were also attenuated in CCR1KO, CCR5KO, or CCL3KO mice (Fig. 6B). Lymphocytes expressing the cell proliferation marker Ki67 were increased in the paracortical areas of the draining lymph nodes of GCV-treated WT mice compared with the other groups (Fig. 6C and Supplemental Fig. 5). Injection of BNL-tk cells marginally increased the proportion of activated $CD4^+$ T cells, defined as $CD44^{hi}CD62L^{lo}CD4^+$, in the draining lymph nodes. Coinjec-

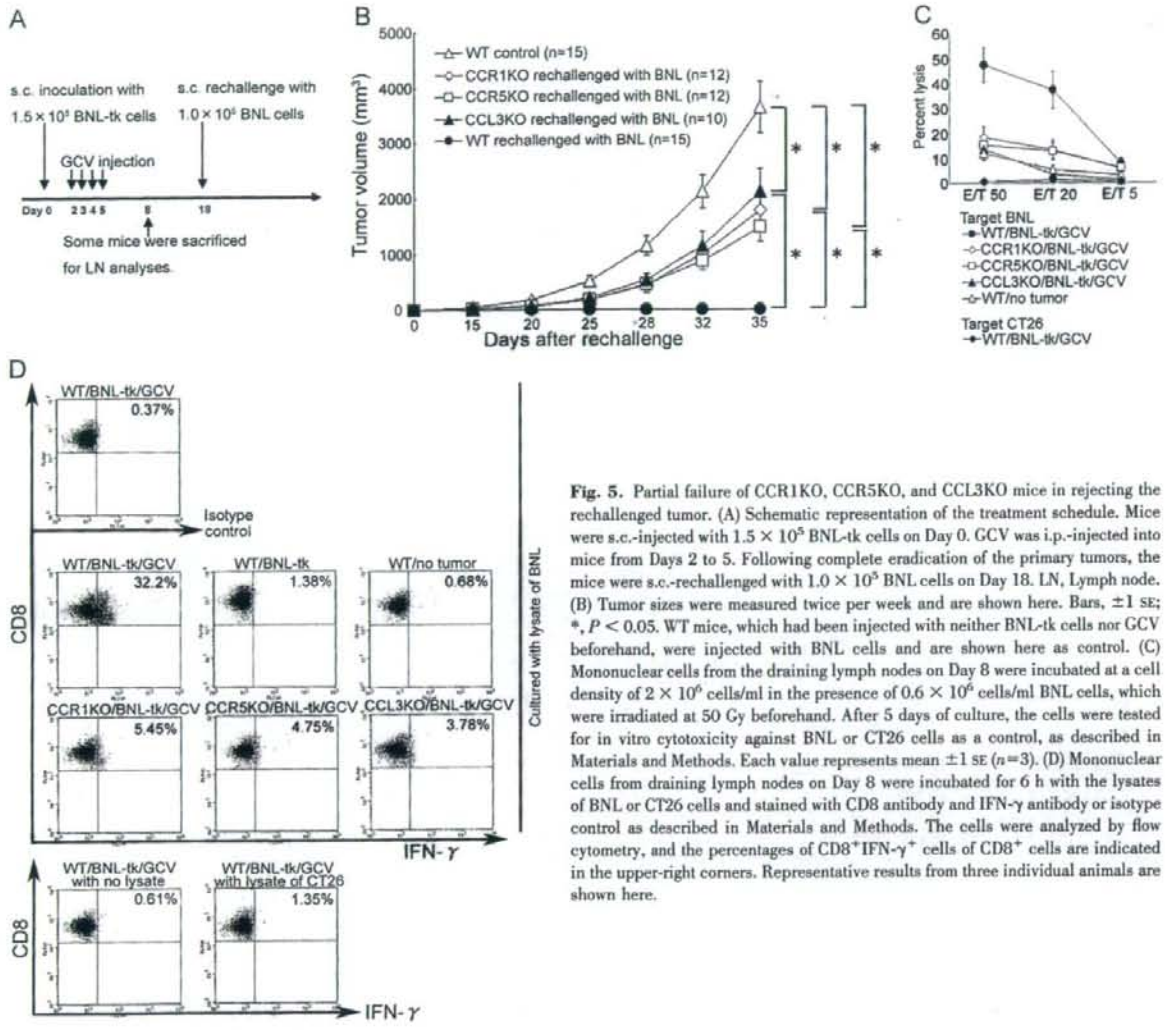

Fig. 5. Partial failure of CCR1KO, CCR5KO, and CCL3KO mice in rejecting the rechallenged tumor. (A) Schematic representation of the treatment schedule. Mice were s.c.-injected with 1.5×10^5 BNL-tk cells on Day 0. GCV was i.p.-injected into mice from Days 2 to 5. Following complete eradication of the primary tumors, the mice were s.c.-rechallenged with 1.0×10^5 BNL cells on Day 18. LN, Lymph node. (B) Tumor sizes were measured twice per week and are shown here. Bars, ±1 SE; *, $P < 0.05$. WT mice, which had been injected with neither BNL-tk cells nor GCV beforehand, were injected with BNL cells and are shown here as control. (C) Mononuclear cells from the draining lymph nodes on Day 8 were incubated at a cell density of 2×10^6 cells/ml in the presence of 0.6×10^6 cells/ml BNL cells, which were irradiated at 50 Gy beforehand. After 5 days of culture, the cells were tested for in vitro cytotoxicity against BNL or CT26 cells as a control, as described in Materials and Methods. Each value represents mean ±1 SE ($n = 3$). (D) Mononuclear cells from draining lymph nodes on Day 8 were incubated for 6 h with the lysates of BNL or CT26 cells and stained with CD8 antibody and IFN-γ antibody or isotype control as described in Materials and Methods. The cells were analyzed by flow cytometry, and the percentages of $CD8^+IFN\text{-}\gamma^+$ cells of $CD8^+$ cells are indicated in the upper-right corners. Representative results from three individual animals are shown here.

tion of GCV further augmented this increment in WT mice but not in KO mice (Fig. 6, D and E). These observations suggest that the absence of CCR1, CCR5, or CCL3 impaired the GCV-induced migration of DCs into the draining lymph nodes and the subsequent proliferation and activation of T cells in the draining lymph nodes.

Restoration of anti-tumor response of KO mice by adoptive transfer of DCs harvested from GCV-treated WT mice

Given the proposed, crucial role of DCs in evoking antitumor immunity after tumor apoptosis, we finally performed adoptive transfer of DCs harvested from the draining lymph nodes of GCV-treated WT mice into the KO mice. DCs were harvested from the draining lymph nodes of GCV-treated, tumor-bearing or tumor-free WT mice and were transferred s.c. into the KO mice on Day 8 (Fig. 5A). The KO mice completely rejected the rechallenged cells when DCs were transferred from GCV-treated, tumor-bearing WT mice but not tumor-free WT mice (**Fig. 7**). These observations suggest that GCV-induced tumor apoptosis mediated the trafficking of DCs to the draining lymph nodes, which can induce the establishment of specific immunity in a CCR1-, CCR5-, or CCL3-dependent manner.

DISCUSSION

Apoptosis was previously presumed to be immunologically silent or even tolerogenic [27]. However, recent reports have indicated that tumor cell apoptosis can induce antitumor immune responses effectively, as the immunogenicity of apoptotic tumor cells is dependent on apoptosis inducers. Indeed, gemcitabine-induced apoptosis can augment cross-priming of tumor-specific $CD8^+$ T cells in vivo rather than cross-tolerizing [8]. Similarly, apoptosis induced by local radiation therapy can generate tumor antigen-specific effector cells that migrate to

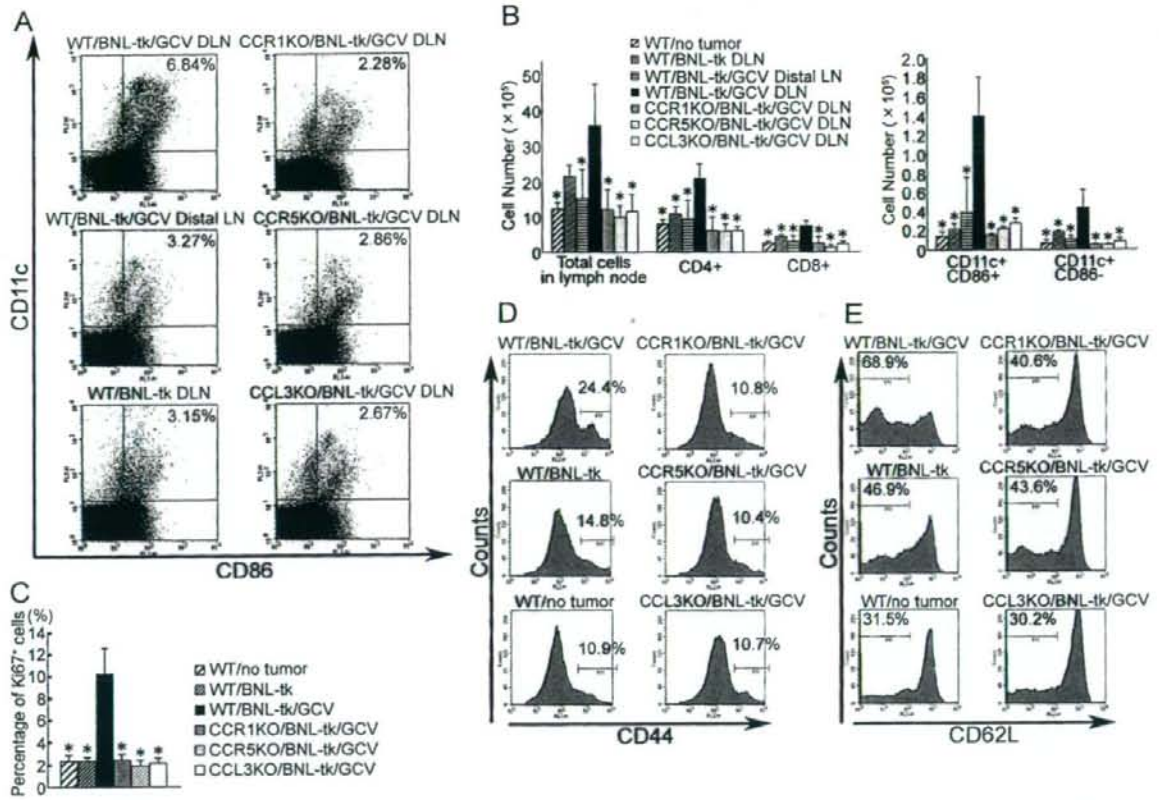

Fig. 6. Apoptosis-induced migration of DCs to the draining lymph nodes (DLN) and intranodal T cell proliferation and activation in a CCR1-, CCR5-, and/or CCL3-dependent manner. Mice were treated according to the schedule shown in Figure 5A. (A) Draining lymph nodes or distal lymph nodes were harvested on Day 8 as indicated in Figure 5A. Mononuclear cells were stained with a combination of FITC-labeled anti-CD86 and PE-labeled anti-CD11c antibodies. The percentage of $CD11c^+CD86^+$ cells was determined and is indicated in the upper-right corners. Representative results from three individual animals are shown here. (B) Absolute cell numbers of each cell population in the draining lymph nodes or distal lymph nodes on Day 8 were determined as described in Materials and Methods. Error bars, ±1 SD; *, $P < 0.05$, compared with draining lymph nodes derived from WT mice treated with BNL-tk/GCV. (C) Draining lymph nodes harvested on Day 8 were immunostained with anti-Ki67 antibody, and percentages of $Ki67^+$ cells in lymph nodes were determined. Error bars, ±1 SD; *, $P < 0.05$, compared with draining lymph nodes derived from WT mice treated with BNL-tk/GCV. (D and E) Mononuclear cells harvested on Day 8 were stained with a combination of FITC-labeled anti-CD4 and PE-labeled anti-CD44 (D) or PE-labeled anti-CD62L (E) antibodies. Histograms were gated on CD4-positive cells, and percentages of $CD44^{hi}$ (D) or $CD62L^{lo}$ (E) cells were determined. Representative results from three individual animals are shown here.

the tumor [28]. Moreover, apoptotic change caused by anthracyclin can induce the translocation of calreticulin to the apoptotic tumor cell surface, and calreticulin exposure can enhance the immunogenicity of apoptotic cancer cells [6, 7]. Thus, apoptosis induced by these measures is sufficiently immunogenic to prevent tumor progression.

The combination of HSV-tk gene transfer and GCV can efficiently induce the apoptosis of the transfected tumors as observed in the present study. Here, we also observed that the treatment augmented the immune response, as evidenced by an increase in the number of tumor-infiltrating DCs. Subsequently, the number of DCs in the draining lymph nodes increased together with enhanced, specific immunity to the injected tumor. These observations suggest that tumor apoptosis induced by HSV-tk/GCV treatment is effective in generating specific tumor immunity, similar to that observed in the case of anticancer drug treatment.

Consistent with our present observations, CCL3 and its related chemokine CCL5 were detected in macrophages infiltrating human cancer tissues [29, 30]. Given their potent chemotactic activity against various types of immune cells [31], gene transfer of CCL3 or CCL5 induced the accumulation of immune cells including DCs, T cells, macrophages, and NK cells in the tumor sites, resulting in delayed tumor growth and prolonged survival [16, 32–34]. Moreover, combination therapy of the HSV-tk and CCL3/CCL20 gene induces an exaggerated accumulation of DCs, $CD4^+$ cells, $CD8^+$ cells, NK cells, and macrophages in the tumor sites compared with HSV-tk/GCV treatment alone, and the net effects are tumor regression and prolonged survival [34]. However, the roles of endogenously produced CCL3 and its related chemokines in tumor apoptosis still remain to be elucidated.

In human HCC, tumor-infiltrating lymphocytes express high levels of CCR5 and CXCR3. Moreover, these lymphocytes

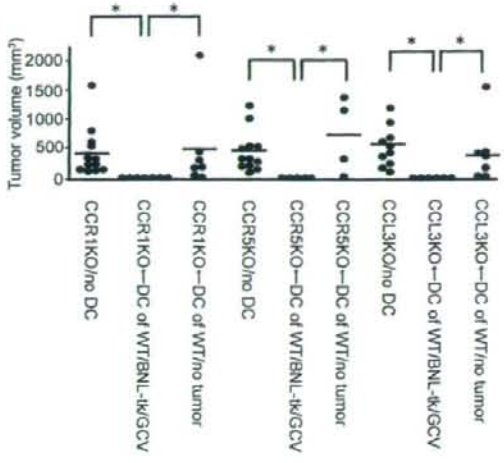

Fig. 7. Adoptive transfer of DCs harvested from GCV-treated WT mice restored the antitumor response of KO mice. After inoculation of BNL-tk tumors, CCR1KO, CCR5KO, or CCL3KO mice were treated with GCV from Days 2 to 5 as described in Figure 5A. The DCs were then harvested from the draining lymph nodes of GCV-treated WT mice and transferred s.c. into the KO mice on Day 8 as shown in Figure 5A. On Day 18, these mice were injected again with parental BNL cells, and tumor sizes were measured on Day 28. GCV-treated KO mice, transferred without or with DCs of naïve WT mice, were also rechallenged with parental BNL cells as control. Bars, mean; *, $P < 0.05$.

show strong chemotactic responses to CC and CXC chemokines including CCL3, CCL4, and CXCL9 [35]. Additional treatments are nevertheless required to enhance the immune responses, as the CCR5- or CXCR3-positive lymphocytes are insufficient to evoke immune responses and eradicate tumor tissues. We demonstrated that suicide gene therapy-induced tumor cell apoptosis augments CCR1- and CCR5-positive cell infiltration into the hepatoma tissues. Further, these CCR1- or CCR5-positive cells are DCs and/or T cells—the cells indispensable for tumor immunity. Thus, suicide gene therapy can potentially enhance tumor immunity by attracting these immune cells to the apoptotic tumor cells.

The initial step leading to specific tumor immunity is the capture of tumor antigens by macrophages and immature DCs, both of which accumulate in tumor sites. However, in this model, CCR1KO, CCR5KO, and CCL3KO mice failed to completely eliminate the rechallenged tumor cells along with reduced intratumoral accumulation of DCs but not F4/80-positive macrophages. These observations suggest that the establishment of specific tumor immunity requires intratumoral recruitment of immature DCs but not macrophages. Activated NK cells can also induce DC maturation in lymphoid organs as well as in nonlymphoid tissues. Although NK cells express chemokine receptors such as CCR5 [36], the deficiency of CCR1 or CCR5 has little effects on intratumoral infiltration of NK cells. These observations preclude the crucial role of NK cells in the establishment of specific tumor immunity in this model.

Immature DCs use several chemokine receptors including CCR1, CCR2, CCR4, CCR5, CCR6, CCR8, and CXCR4 for their migration [22]. However, the chemokine receptor(s) regulating immature DC trafficking to tumor sites still need(s) to be determined. We previously observed that CCL3 induced mobilization of DC precursors into circulation [37] and detected CCL3 in tumor-infiltrating $CD3^+$ T cells and macrophages after GCV treatment. Therefore, we investigated the roles of CCL3 and its receptors CCR1 and CCR5 in the intratumoral recruitment of DCs and the subsequent establishment of specific tumor immunity. Although CCL4 and CCL5 expression was augmented along with CCL3 expression in tumor sites, the deletion of the *CCL3* gene alone markedly reduced the DC migration, intranodal T cell accumulation, and subsequent Th1 cytokine expression. Similarly, deletion of the *CCL3* gene alone prevented coxsackievirus-induced myocarditis [38], despite enhanced, intracardiac expression of CCL3, CCL4, and CCL5 mRNA [39]. Thus, these three chemokines may form a positive feedback loop, and the deletion of either chemokine might reduce the expression of the others. Moreover, the lack of CCR1 or CCR5 reduces the migration of DCs to tumor sites and subsequent tumor immunity in the draining lymph nodes, such as DC and T cell accumulation and Th1 cytokine expression. As almost all CD11c- and DEC205-positive DCs express CCR1 and CCR5, DC migration may require coordinated and synergistic actions of both of these chemokine receptors.

We have provided definitive evidence regarding the essential contribution of CCL3 and its receptors to apoptosis-induced, specific tumor immunity, which exert their role by attracting DCs to tumor tissues. These observations further suggest that specific tumor immunity can be established more efficiently if some techniques such as chemokine gene transfer can augment the recruitment of immature DCs to apoptotic tumor tissues caused by chemotherapeutic agents and/or irradiation as well as suicide gene therapy.

ACKNOWLEDGMENTS

We thank Dr. Philip M. Murphy (NIAID, NIH) for providing us with CCR1KO mice. We also thank Dr. Toshikazu Kondo (Wakayama Medical University, Wakayama, Japan) for his technical advice about double-color immunofluorescence analysis.

REFERENCES

1. Tsukuma, H., Hiyama, T., Tanaka, S., Nakao, M., Yabuuchi, T., Kitamura, T., Nakanishi, K., Fujimoto, I., Inoue, A., Yamazaki, H., Kawashima, T. (1993) Risk factors for hepatocellular carcinoma among patients with chronic liver disease. *N. Engl. J. Med.* **328**, 1797–1801.
2. Velázquez, R. F., Rodríguez, M., Navascués, C. A., Linares, A., Pérez, R., Sotorríos, N. G., Martínez, I., Rodrigo, L. (2003) Prospective analysis of risk factors for hepatocellular carcinoma in patients with liver cirrhosis. *Hepatology.* **37**, 520–527.
3. Okita, K. (2006) Management of hepatocellular carcinoma in Japan. *J. Gastroenterol.* **41**, 100–106.
4. Poon, R. T., Fan, S. T., Ng, I. O., Lo, C. M., Liu, C. L., Wong, J. (2000) Different risk factors and prognosis for early and late intrahepatic recurrence after resection of hepatocellular carcinoma. *Cancer* **89**, 500–507.
5. Butterfield, L. H. (2004) Immunotherapeutic strategy for hepatocellular carcinoma. *Gastroenterology* **127**, S232–S241.
6. Obeid, M., Tesniere, A., Ghiringhelli, F., Fimia, G. M., Apetoh, L., Perfettini, J. L., Castedo, M., Mignot, G., Panaretakis, T., Casares, N.,

Métivier, D., Larochette, N., van Endert, P., Ciccosanti, F., Piacentini, M., Zitvogel, L., Kroemer, G. (2007) Calreticulin exposure dictates the immunogenicity of cancer cell death. *Nat. Med.* **13,** 54–61.
7. Casares, N., Pequignot, M. O., Tesniere, A., Ghiringhelli, F., Roux, S., Chaput, N., Schmitt, E., Hamai, A., Hervas-Stubbs, S., Obeid, M., Coutant, F., Métivier, D., Pichard, E., Aucouturier, P., Pierron, G., Garrido, C., Zitvogel, L., Kroemer, G. (2005) Caspase-dependent immunogenicity of doxorubicin-induced tumor cell death. *J. Exp. Med.* **202,** 1691–1701.
8. Nowak, A. K., Lake, R. A., Marzo, A. L., Scott, B., Heath, W. R., Collins, E. J., Frelinger, J. A., Robinson, B. W. S. (2003) Induction of tumor cell apoptosis in vivo increases tumor antigen cross-presentation, cross-priming rather than cross-tolerizing host tumor-specific CD8 T cells. *J. Immunol.* **170,** 4905–4913.
9. Hamel, W., Magnelli, L., Chiarugi, V. P., Israel, M. A. (1996) Herpes simplex virus thymidine kinase/ganciclovir-mediated apoptotic death of bystander cells. *Cancer Res.* **56,** 2697–2702.
10. Beltinger, C., Fulda, S., Kammertoens, T., Meyer, E., Uckert, W., Debatin, K. M. (1999) Herpes simplex virus thymidine kinase/ganciclovir-induced apoptosis involves ligand-independent death receptor aggregation and activation of caspases. *Proc. Natl. Acad. Sci. USA* **96,** 8699–8704.
11. Freeman, S. M., Ramesh, R., Marrogi, A. J. (1997) Immune system in suicide-gene therapy. *Lancet* **349,** 2–3.
12. Vile, R. G., Castleden, S., Marshall, J., Camplejohn, R., Upton, C., Chong, H. (1997) Generation of an anti-tumor immune response in a non-immunogenic tumor: HSVtk killing in vivo stimulates a mononuclear cell infiltrate and a Th1-like profile of intratumoural cytokine expression. *Int. J. Cancer* **71,** 267–274.
13. Freeman, S. M., Ramesh, R., Shastri, M., Munshi, A., Jensen, A. K., Marrogi, A. J. (1995) The role of cytokines in mediating the bystander effect using HSV-TK xenogeneic cells. *Cancer Lett.* **92,** 167–174.
14. Chen, S. H., Chen, X. H. L., Wang, Y., Kosai, K., Finegold, M. J., Rich, S. S., Woo, S. L. C. (1995) Combination gene therapy for liver metastasis of colon carcinoma in vivo. *Proc. Natl. Acad. Sci. USA* **92,** 2577–2581.
15. Chen, S. H., Kosai, K., Xu, B., Pham-Nguyen, K., Contant, C., Finegold, M. J., Woo, S. L. C. (1996) Combination suicide and cytokine gene therapy for hepatic metastases of colon carcinoma: sustained antitumor immunity prolongs animal survival. *Cancer Res.* **56,** 3758–3762.
16. Tsuchiyama, T., Nakamoto, Y., Sakai, Y., Marukawa, Y., Kitahara, M., Mukaida, N., Kaneko, S. (2007) Prolonged, NK cell-mediated antitumor effects of suicide gene therapy combined with monocyte chemoattractant protein-1 against hepatocellular carcinoma. *J. Immunol.* **178,** 574–583.
17. Banchereau, J., Steinman, R. M. (1998) Dendritic cells and the control of immunity. *Nature* **392,** 245–252.
18. Sallusto, F., Lanzavecchia, A. (1999) Mobilizing dendritic cells for tolerance, priming, and chronic inflammation. *J. Exp. Med.* **189,** 611–614.
19. Castellino, F., Huang, A. Y., Altan-Bonnet, G., Stoll, S., Scheinecker, C., Germain, R. N. (2006) Chemokines enhance immunity by guiding naïve $CD8^+$ T cells to sites of $CD4^+$ T cell-dendritic cell interaction. *Nature* **440,** 890–895.
20. Dieu, M. C., Vanbervliet, B., Vicari, A., Bridon, J. M., Oldham, E., Aït-Yahia, S., Brière, F., Zlotnik, A., Lebecque, S., Caux, C. (1998) Selective recruitment of immature and mature dendritic cells by distinct chemokines expressed in different anatomic sites. *J. Exp. Med.* **188,** 373–386.
21. Sozzani, S., Luini, W., Borsatti, A., Polentarutti, N., Zhou, D., Piemonti, L., D'Amico, G., Power, C. A., Wells, T. N. C., Gobbi, M., Allavena, P., Mantovani, A. (1997) Receptor expression and responsiveness of human dendritic cells to a defined set of CC and CXC chemokines. *J. Immunol.* **159,** 1993–2000.
22. Sozzani, S. (2005) Dendritic cell trafficking: more than just chemokines. *Cytokine Growth Factor Rev.* **16,** 581–592.
23. Murai, M., Yoneyama, H., Ezaki, T., Suematsu, M., Terashima, Y., Harada, A., Hamada, H., Asakura, H., Ishikawa, H., Matsushima, K. (2003) Peyer's patch is the essential site in initiating murine acute and lethal graft-versus-host reaction. *Nat. Immunol.* **4,** 154–160.
24. Tsuchiyama, T., Kaneko, S., Nakamoto, Y., Sakai, Y., Honda, M., Mukaida, N., Kobayashi, K. (2003) Enhanced antitumor effects of a bicistronic adenovirus vector expressing both herpes simplex virus thymidine kinase and monocyte chemoattractant protein-1 against hepatocellular carcinoma. *Cancer Gene Ther.* **10,** 260–269.
25. Murai, M., Yoneyama, H., Harada, A., Yi, Z., Vestergaard, C., Guo, B., Suzuki, K., Asakura, H., Matsushima, K. (1999) Active participation of $CCR5^+CD8^+$ T lymphocytes in the pathogenesis of liver injury in graft-versus-host disease. *J. Clin. Invest.* **104,** 49–57.
26. Lu, P., Nakamoto, Y., Nemoto-Sakai, Y., Fujii, C., Wang, H., Hashii, M., Ohmoto, Y., Kaneko, S., Kobayashi, K., Mukaida, N. (2003) Potential interaction between CCR1 and its ligand, CCL3, induced by endogeneously produced interleukin-1 in human hepatomas. *Am. J. Pathol.* **162,** 1249–1258.
27. Steinman, R. M., Turley, S., Mellman, I., Inaba, K. (2000) The induction of tolerance by dendritic cells that have captured apoptotic cells. *J. Exp. Med.* **191,** 411–416.
28. Lugade, A. A., Moran, J. P., Gerber, S. A., Rose, R. C., Frelinger, J. G., Lord, E. M. (2005) Local radiation therapy of B16 melanoma tumors increases the generation of tumor antigen-specific effector cells that traffic to the tumor. *J. Immunol.* **174,** 7516–7523.
29. Tang, K. F., Tan, S. Y., Chan, S. H., Chong, S. M., Loh, K. S., Tan, L. K. S., Hu, H. (2001) A distinct expression of CC chemokines by macrophages in nasopharyngeal carcinoma: implication for the intense tumor infiltration by T lymphocytes and macrophages. *Hum. Pathol.* **32,** 42–49.
30. Musha, H., Ohtani, H., Mizoi, T., Kinouchi, M., Nakayama, T., Shiiba, K., Miyagawa, K., Nagura, H., Yoshie, O., Sasaki, I. (2005) Selective infiltration of $CCR5^+CXCR3^+$ T lymphocytes in human colorectal carcinoma. *Int. J. Cancer* **116,** 949–956.
31. Menten, P., Wuyts, A., van Damme, J. (2002) Macrophage inflammatory protein-1. *Cytokine Growth Factor Rev.* **13,** 455–481.
32. Lavergne, E., Combadière, C., Iga, M., Boissonnas, A., Bonduelle, O., Maho, M., Debré, P., Combadiere, B. (2004) Intratumoral CC chemokine ligand 5 overexpression delays tumor growth and increases tumor cell infiltration. *J. Immunol.* **173,** 3755–3762.
33. Fushimi, T., Kojima, A., Moore, M. A., Crystal, R. G. (2000) Macrophage inflammatory protein 3α transgene attracts dendritic cells to established murine tumors and suppresses tumor growth. *J. Clin. Invest.* **105,** 1383–1393.
34. Crittenden, M., Gough, M., Harrington, K., Olivier, K., Thompson, J., Vile, R. G. (2003) Expression of inflammatory chemokines combined with local tumor destruction enhances tumor regression and long-term immunity. *Cancer Res.* **63,** 5505–5512.
35. Yoong, K. F., Afford, S. C., Jones, R., Aujla, P., Qin, S., Price, K., Hubscher, S. G., Adams, D. H. (1999) Expression of CXC and CC chemokines in human malignant liver tumors: a role for human monokine induced by γ-interferon in lymphocyte recruitment to hepatocellular carcinoma. *Hepatology* **30,** 100–111.
36. Walzer, T., Dalod, M., Robbins, S. H., Zitvogel, L., Vivier, E. (2005) Natural-killer cells and dendritic cells: "l'union fait la force". *Blood* **106,** 2252–2258.
37. Zhang, Y., Yoneyama, H., Wang, Y., Ishikawa, S., Hashimoto, S., Gao, J. L., Murphy, P. M., Matsushima, K. (2004) Mobilization of dendritic cell precursors into the circulation by administration of MIP-1α in mice. *J. Natl. Cancer Inst.* **96,** 201–209.
38. Cook, D. N., Beck, M. A., Coffman, T. M., Kirby, S. L., Sheridan, J. F., Pragnell, I. B., Smithies, O. (1995) Requirement for an inflammatory response to viral infection. *Science* **269,** 1583–1585.
39. Gebhard, J. R., Perry, C. M., Harkins, S., Lane, T., Mena, I., Asensio, V. C., Campbell, I. L., Whitton, J. L. (1998) Coxsackievirus B3-induced myocarditis. Perforin exacerbates disease, but plays no detectable role in virus clearance. *Am. J. Pathol.* **153,** 417–428.

ELSEVIER

Journal of Hepatology 49 (2008) 946–954

Journal of Hepatology

www.elsevier.com/locate/jhep

Expression of multidrug resistance-associated protein 3 and cytotoxic T cell responses in patients with hepatocellular carcinoma☆

Eishiro Mizukoshi, Masao Honda, Kuniaki Arai, Tatsuya Yamashita, Yasunari Nakamoto, Shuichi Kaneko*

Department of Gastroenterology, Graduate School of Medicine, Kanazawa University, Kanazawa, Ishikawa 920-8641, Japan

***Background/Aims*: Multidrug resistance-associated protein 3 (MRP3) is a carrier-type transport protein belonging to the ABC transporters. It is expressed in normal tissues, and enhanced expression in many cancers has been reported. In this study, we investigated the usefulness of MRP3 as a target antigen in immunotherapy for hepatocellular carcinoma (HCC).**

***Methods*: The MRP3 expression level in HCC tissue was measured by quantitative PCR. MRP3-specific T cell responses were investigated by several immunological techniques using peripheral blood mononuclear cells or tumor-infiltrating lymphocytes.**

***Results*: The MRP3 expression level in HCC tissue was significantly higher than that in non-cancerous tissue ($P < 0.05$). MRP3-specific cytotoxic T cells (CTLs) could be induced regardless of liver function, the presence or absence of HCV infection, the blood AFP level, and the stage of HCC. The CTLs showed cytotoxicity against HCC cells overexpressing MRP3. A negative correlation was present between the MRP3 expression level in HCC tissue and the frequency of MRP3-specific CTLs. The frequency of MRP3-specific CTLs increased after HCC treatment, such as transcatheter arterial embolization and radiofrequency ablation.**

***Conclusions*: Our study demonstrates that MRP3 is a potential candidate for tumor antigen with strong immunogenicity in HCC immunotherapy.**

Keywords: **Immune response; CD8; HLA-A24; Hepatitis; Cancer**

1. Introduction

Hepatocellular carcinoma (HCC) is treatable by hepatectomy or percutaneous ablation when the lesion is localized to some extent, and radical therapeutic effects can be obtained when the resection or cauterization with a safety margin can be performed [1,2]. However, active hepatitis and cirrhosis in the surrounding non-tumor liver tissues exhibit high carcinogenetic potentials to develop *de novo* HCC, and therefore, the recurrence rate of HCC after treatment is very high [3,4].

To protect against recurrence, tumor antigen-specific immunotherapy is an attractive strategy. For the development of HCC-specific immunotherapy and analysis of immune responses to the treatment, the identification of HCC-specific tumor antigens or their antigenic epitopes is necessary. However, only a few HCC-specific tumor antigens and their antigenic epitopes have been identified [5–10].

MRP3 is a carrier-type transport protein belonging to the ABC transporters that transport substances against

Received 11 January 2008; received in revised form 23 April 2008; accepted 7 May 2008; available online 5 June 2008
Associate Editor: V. Barnaba

☆ The authors declare that they do not have anything to disclose regarding funding from industries or conflict of interest with respect to this manuscript.

* Corresponding author. Tel.: +81 76 265 2230; fax: +81 76 234 4250.
E-mail address: skaneko@m-kanazawa.jp (S. Kaneko).

Abbreviations: HLA, human leukocyte antigen; IFN, interferon; PBMC, peripheral blood mononuclear cell; TIL, tumor-infiltrating lymphocytes; HCV, hepatitis C virus; ELISPOT, enzyme linked immunospot.

0168-8278/$34.00
doi:10.1016/j.jhep.2008.05.012

the concentration gradient in an ATP energy-dependent manner [11]. It is expressed at a high level in the small and large intestine, pancreas, placenta, and adrenal cortex [12], and recent studies have reported that its expression is enhanced in various cancer cells [13–15]. Yamada et al. demonstrated that MRP3 was a tumor rejection antigen recognized by cytotoxic T cells (CTLs), using lymphocytes infiltrating into lung adenocarcinoma, and identified its CTL epitope [13]. These reports suggest that MRP3 may be useful as a target antigen in HCC immunotherapy. However, the MRP3 expression level in HCC tissue has been controversial [16,17], and the association between the expression level and the degree of the immune response to MRP3 in HCC patients has not been clarified.

In this study, we measured the MRP3 expression level in various hematoma cell lines and HCC tissues in HCC patients, and analyzed immune responses to MRP3 using peripheral blood mononuclear cells (PBMCs) and tumor-infiltrating lymphocytes (TILs) to investigate the usefulness of MRP3 in HCC immunotherapy.

2. Materials and methods

2.1. Patients

This study examined 103 HLA-A24-positive patients with HCC (Table 1). All subjects were negative for Abs to human immunodeficiency virus (HIV), and gave written informed consent to participate in this study in accordance with the Helsinki declaration. The diagnosis of HCC was histologically confirmed by taking US-guided needle biopsy specimens in 35 cases, surgical resection in 13 cases, and autopsy in 4 cases. For the remaining 51 patients, the diagnosis was based on typical hypervascular tumor staining on angiography in addition to typical findings, which showed hyperattenuated areas in the early phase and hypoattenuation in the late phase on dynamic CT [18]. Eleven healthy blood donors with HLA-A24, who did not have a history of cancer and were negative for HBsAg and anti-HCVAb, served as controls.

2.2. Laboratory and virologic testing

Blood samples were tested for HBsAg and HCVAb by commercial immunoassays (Fuji Rebio, Tokyo, Japan). HLA-based typing of PBMC from patients and normal donors was performed as previously described [10].

The serum AFP level was measured by enzyme immunoassay (AxSYM AFP, Abbott Japan, Tokyo, Japan) and the pathological grading of tumor cell differentiation was assessed according to the general rules for the clinical and pathologic study of primary liver cancer [19]. The severity of liver disease (stage of fibrosis) was evaluated according to the criteria of Desmet et al. [20] using biopsy specimens of liver tissue, where F4 was defined as cirrhosis.

2.3. Cell lines

Eight human hepatoma cell lines: HepG2, Alex, Huh6, HLE, HLF, Hep3B, SKHep1, and Huh7, were cultured in DMEM (Gibco, Grand Island, NY, USA) with 10% fetal calf serum (FCS) (Gibco, Grand Island, NY, USA). The HLA-A*2402 gene-transfected C1R cell line (C1R-A24) [21] was cultured in RPMI 1640 medium containing 10% FCS and 500 μg/ml of hygromycin B (Sigma, St. Louis, MO, USA), and K562 was cultured in RPMI 1640 medium containing 10% FCS.

2.4. Quantitative real time detection (RTD)-PCR

We performed quantitative RTD-PCR using TaqMan Universal Master Mix (PE Applied Biosystems, Foster City, CA, USA). Primer pairs and probes for MRP3 and β-actin were obtained from TaqMan assay reagents library. Total RNA was isolated from cell lines and liver tissue samples using an RNA extraction kit (Micro RNA Extraction Kit, Stratagene, La Jolla, CA, USA). We reverse-transcribed 1 μg of isolated RNA to cDNA using SuperScript® II RT (Invitrogen, Carlsbad, CA, USA) according to the manufacturer's instructions, and the resultant cDNA was amplified with appropriate TaqMan assay reagents as previously described [22].

2.5. Preparation of PBMCs and TILs

PBMCs and TILs were isolated as previously described [9]. Fresh PBMCs were used for the CTL induction, and the remaining PBMCs and TILs were resuspended in RPMI 1640 medium containing 80% FCS and 10% dimethyl sulfoxide and cryopreserved until used. In patients with treatment, PBMCs were obtained before and 2–4 weeks after the treatment.

2.6. CTL induction and cytotoxicity assay

Peptides $MRP3_{503}$, $MRP3_{692}$, and $MRP3_{765}$, which were identified to contain a HLA-A24 restricted CTL epitope [13], were used for the induction of MRP3-specific T cells (Table 2). Peptides were synthesized at Mimotope (Melbourne, Australia) and Sumitomo Pharmaceuticals (Osaka, Japan). They were identified using mass spectrometry, and their purities were determined to be >80% by analytical HPLC. CTLs were expanded from PBMCs as previously described [23]. Briefly, four hundred thousand cells per well were stimulated with synthetic peptides at 10 μg/ml, 10 ng/ml rIL-7 and 100 pg/ml rIL-12 (Sigma, St. Louis, Mo) in RPMI 1640 supplemented with 10% heat inactivated human AB serum, 100 U/ml penicillin and 100 μg/ml streptomycin. The cultures were re-stimulated with 10 μg/ml peptide, 20 U/ml rIL-2 (Sigma, St. Louis, MO) and 10^5 mytomicin C treated autologous PBMCs on days 7 and 14. On days 3, 10 and 17, 100 μl of RPMI with 10% human AB serum and 10 U/ml rIL-2 (final concentration) was added to each well.

C1R-A24 cells and human hepatoma cell lines were used as target cells. Cytotoxicity assays were performed in at least 10 HCC patients for each peptide as previously described [10]. Spontaneous release

Table 1
Characteristics of the patients studied

Clinical diagnosis	No. of patients	Sex M/F	Age (yr) Mean ± SD	ALT (IU/L) Mean ± SD	AFP (ng/ml) mean ± SD	Etiology (B/C/B + C/Others)	Child Pugh (A/B/C)	Diff. degree[a] (Wel/Mod/ Por/ND)	Tumor size[b] (Large/ Small)	Tumor multiplicity (Multiple/ Solitary)	Vascular Invasion (+/−)	TNM stage (I/II/IIIA/ IIIB/IIIC/IV)
HCC patients	103	79/24	63 ± 10	65 ± 37	3155 ± 15946	19/73/2/9	61/39/3	17/31/4/51	79/24	73/30	30/73	24/51/16/1/3/8
Normal donors	11	8/3	35 ± 2	ND	ND	ND	ND	ND	ND	ND	ND	ND

[a] Histological degree of HCC; wel: well-differentiated, mod: moderately differentiated, por: poorly differentiated, ND: not determined
[b] Tumor size was divided into either 'small' (≦2 cm) or 'large' (>2 cm)

Table 2
Peptides

Peptide	Source	Start position	Amino acid sequence	HLA restriction
$MRP3_{503}$	MRP3	503	LYAWEPSFL	HLA-A24
$MRP3_{692}$	MRP3	692	AYVPQQAWI	HLA-A24
$MRP3_{765}$	MRP3	765	VYSDADIFL	HLA-A24
HIV env_{584}	HIV envelope	584	RYLRDQQLL	HLA-A24
CMV $pp65_{328}$	CMV pp65	328	QYDPVAALF	HLA-A24
AFP_{403}	AFP	403	KYIQESQAL	HLA-A24

was <15% of the maximum release for all experiments. For the assay using hepatoma cell lines, the cytotoxic activity was considered positive when it was higher than that of CTL against K562 which shows non-specific lysis. The assay was performed at least three times for each peptide.

2.7. ELISPOT assay

ELISPOT assays were performed as previously described with the following modifications [9,10]. Peptides $MRP3_{503}$, $MRP3_{692}$, and $MRP3_{765}$ were used for the detection of MRP3-specific T cells. Negative controls consisted of a HIV envelope-derived peptide ($HIVenv_{584}$) [24]. Positive controls consisted of 10 ng/ml phorbol 12-myristate 13-acetate (PMA, Sigma) or a CMV pp65-derived peptide ($CMVpp65_{328}$) [25]. The colored spots were counted with a KS ELISpot Reader (Zeiss, Tokyo, Japan). The number of specific spots was determined by subtracting the number of spots in the absence of antigen from the number of spots in its presence. Responses for peptides $MRP3_{503}$, $MRP3_{692}$, and $MRP3_{765}$ in HCC patients were considered positive if more than the mean + 3SD specific spots in healthy normal donors were detected and if the number of spots in the presence of antigen was at least twofold greater than the number of spots in its absence. Responses for peptides $HIVenv_{584}$ and $CMVpp65_{328}$ were considered positive if more than 10 specific spots were detected and if the number of spots in the presence of antigen was at least twofold greater than the number of spots in the absence of antigen.

2.8. Tetramer staining and flow cytometry

Peptide $MRP3_{765}$ specific tetramer was purchased from Medical Biological Laboratories Co., Ltd (Nagoya, Japan). Tetramer staining was performed according to a previously reported method with several modifications [10]. In brief, PBMCs were stained with CD8-PerCP (BD PharMingen, San Diego, CA, USA) and tetramer-PE (10 μl) for 30 min at room temperature. Cells were washed, fixed with 0.5% paraformaldehyde/PBS, and analyzed on a FACSCalibur™ flow cytometer. Data analysis was undertaken with CELLQuest™ software (Becton–Dickinson, San Jose, CA, USA).

2.9. Statistical analysis

Data are expressed as means ± SD. The χ^2 test with Yates' correction, Fisher's exact probability test, and the unpaired *t*-test were used for statistical analyses where appropriate. Linear regression lines for the relationship between expression of MRP3 mRNA and MRP3-specific immune responses were calculated using Pearson's correlation coefficient. A level of $P < 0.05$ was considered significant.

3. Results

3.1. Patient profile

The clinical profiles of the patients are shown in Table 1. In 52 patients, HCC was histologically classified as well-, moderately, and poorly differentiated HCC in 17, 31, and 4, respectively. In the other patients, HCC was diagnosed based on typical CT findings and AFP elevation. On tumor classification based on the size and number, the tumor was large (>2 cm) in 79, small (≤2 cm) in 24, multiple in 73, and solitary in 30. Vascular invasion was noted in 30 patients. On tumor classification using the TNM staging of the Union Internationale Contre Le Cancer (UICC) classification system (6th version), 24, 51, 16, 1, 3, and 8 patients were staged I, II, IIIA, IIIB, IIIC, and IV, respectively.

3.2. Expression of MRP3 in hepatoma cell lines and HCC tissues

To investigate the MRP3 expression level in HCC, we measured MRP3 mRNA in 8 hepatoma cell lines by real-time PCR. The expression ratio of MRP3 to β-actin, measured as an internal control, is shown in Fig. 1A. All hepatoma cell lines except HLF expressed MRP3, but the expression level varied among the cell lines. HepG2, Hep3B and Huh7 showed high expression levels, but Alex, HLE, SKHep1 and Huh6 showed low expression levels.

The MRP3 expression level in HCC tissues was compared with non-cancerous tissues in specimens obtained from 20 HCC patients by US-guided needle tumor biopsy or surgical resection. The MRP3 expression level was significantly higher in HCC tissue than in the non-cancerous tissue ($P < 0.05$) (Fig. 1B). In the analysis of the individual MRP3 expression levels, 11 of 20 (55%) HCC tissues showed higher expression level than that of Huh 7 whose average of expression level is 1.0 (Fig. 1C).

3.3. Cytotoxic activity of MRP3 peptide-specific CTL against hepatoma cell lines

Whether the MRP3-derived peptides used were capable of inducing peptide-specific CTL from PBMCs was investigated in at least 10 HCC patients. The CTLs specific for $MRP3_{503}$, $MRP3_{692}$, and $MRP3_{765}$ were induced in 3, 3 and 2 patients, respectively. As shown in Fig. 2A, all CTL induced with $MRP3_{503}$, $MRP3_{692}$, and $MRP3_{765}$ showed high-level cytotoxicity against C1RA24 cells pulsed with the corresponding peptides.

These CTLs exhibited cytotoxicity against hepatoma cell lines with the HLA-A24 molecule and high expression of MRP3, HepG2 and HLE, but not against MRP3-hypoexpressing Huh6 and MRP3-overexpressing Huh7 without HLA-A24 molecule (Fig. 2B).

3.4. T Cell responses to MRP3-derived peptides assessed by IFN-γ ELISPOT analysis

To determine a significant number of T cells that specifically reacted with $MRP3_{503}$, $MRP3_{692}$ and $MRP3_{765}$

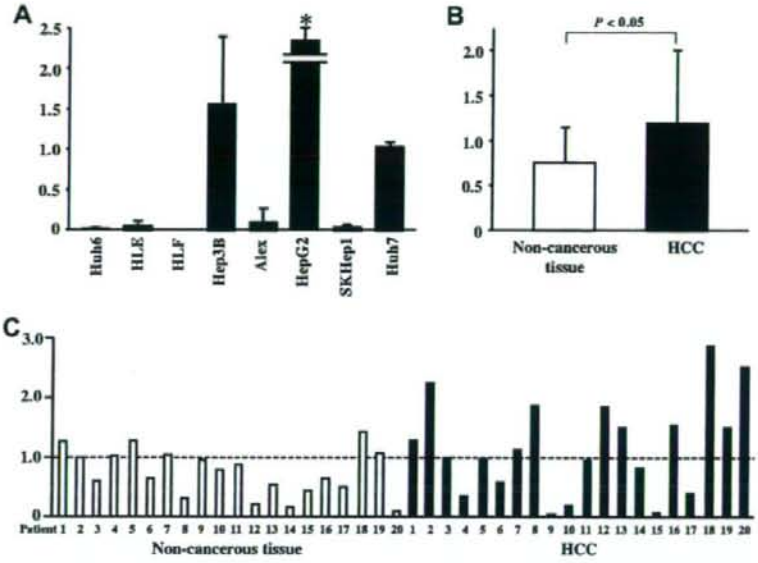

Fig. 1. Expression levels of MRP3 mRNA. (A) Expression of MRP3 mRNA was measured by real-time PCR in hepatoma cell lines. (B) Comparison of MRP3 mRNA expression levels between non-tumor (white bar) and tumor (solid bar) tissues. The data are expressed as means + SD. The unpaired *t*-test was used for a statistical analysis. (C) Comparison of MRP3 mRNA expression levels between non-tumor (white bar) and tumor (solid bar) tissues in individual HCC patients. * denotes 6.15 + 4.21.

peptides in HCC patients, ELISPOT assays were performed using PBMCs from 11 healthy donors. The number of specific spots was 0.2 ± 0.5, 1.5 ± 2.1, 0.9 ± 1.0, 1.3 ± 2.0, and 13.3 ± 15.7 cells/3×10^5 PBMCs, respectively (Fig. 3). Similarly, cells that specifically reacted with the peptides were counted in HCC patient-derived PBMCs. Regarding a number of T cells that specifically reacted with the peptide of larger than the mean + 3SD of that in healthy donor-derived PBMCs as a significant response, 20.0, 14.1, and 21.4% of the patients showed significant responses to $MRP3_{503}$, $MRP3_{692}$, and $MRP3_{765}$, respectively (Fig. 4A). A significant response specific for $CMVpp65_{328}$ was detected in 51.0% and 36.4% of the HCC patients and healthy donors, respectively, showing no significant difference between the 2 groups. On the other hand, no significant response for $HIVenv_{584}$ was observed in both groups.

On similar analysis of TIL, 75.0, 75.0, and 37.5% of the patients showed significant responses to $MRP3_{503}$, $MRP3_{692}$, and $MRP3_{765}$, respectively, revealing that the frequencies were higher than those in PBMCs (Fig. 4B).

3.5. Detection of $MRP3_{765}$ tetramer$^+$ and CD8$^+$ T lymphocytes in PBMCs

The frequency of MRP3-specific T cells was also investigated using $MRP3_{765}$ tetramer in 20 HCC patients. To confirm the specificity of $MRP3_{765}$ tetramer, we tried to detect the tetramer$^+$ cells in a CTL line induced by stimulation with $MRP3_{765}$ peptide. The frequency of $MRP3_{765}$ tetramer$^+$ cells in CD8$^+$ cells was increased from 0.03% before to 9.15% after stimulation (Fig. 5A). When PBMC was stimulated with irrelevant peptide (AFP_{403}), the frequency of $MRP3_{765}$ tetramer$^+$ cells was only 0.08%.

To count the frequency of tetramer$^+$ cells in peripheral blood, we used freshly isolated non-stimulated PBMCs for the assay. The tetramer$^+$ and CD8$^+$ T cells accounted for 0.00–0.23% in PBMCs of HCC patients (Fig. 5B). Next, the results were compared with those of ELISPOT assay. In patients 1 to 7, both $MRP3_{765}$ tetramer$^+$ and IFN-γ producing cells responding to the peptide in ELISPOT assay were detected. In contrast, in patients 8 to 13, the frequency of tetramer$^+$ cells was high, but no significant increase in the $MRP3_{765}$ peptide-specific T cell count was detected by the ELISPOT assay.

3.6. MRP3-specific T cell responses and clinical features of HCC patients

To clarify the clinical characteristics of MRP3-specific T cell responses in HCC patients, the clinical background was compared between patients who showed positive responses to MRP3-derived peptides on ELISPOT assay and those who did not. No significant differences were noted between the 2 groups (Table 3).

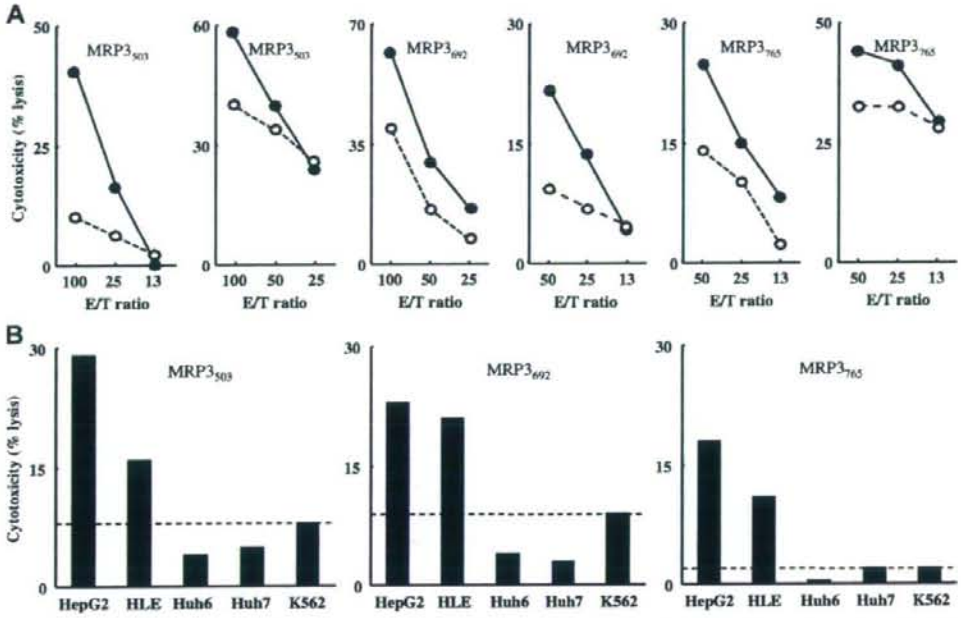

Fig. 2. Cytotoxicity of MRP3-specific T-cell lines derived with peptide in patients with HCC. (A) The cytotoxicity of T-cell lines was determined by a standard 6-h cytotoxicity assay at various effector to target (E/T) ratios against C1R-A*2402 cells pulsed with or without one of the MRP3-derived peptides listed in Table 2. The open circle shows the cytotoxicity against C1R-A*2402 cells pulsed without a peptide. The closed circle shows the cytotoxicity against C1R-A*2402 cells pulsed with a peptide. (B) Cytotoxicity of MRP3-specific T-cell lines derived with peptide was also measured against hepatoma cell lines. The cytotoxicity was considered positive when it was higher than that against K562 which shows non-specific lysis. HepG2 expresses MRP3 and has HLA-A*2402. Huh 6 and HLE show a low expression of MRP3 and have HLA-A*2402. Huh 7 shows MRP3 expression, but does not have HLA-A*2402. Cytotoxicity was determined by a standard 6-h cytotoxic assay (E/T ratio of 50:1).

In 20 HCC patients in whom the MRP3 expression level in HCC tissue could be measured, the relationship between the expression level and frequency of MRP3-specific T cells was investigated. A significant negative correlation was present between the MRP3 expression level in HCC tissue and MRP3-specific T cell frequency ($r = -0.54$, $P < 0.05$) (Fig. 6A). When the relationship between the MRP3 expression level in HCC tissue and CMVpp65-specific T-cell frequency was similarly analyzed, no significant correlation was present. Furthermore, when the patients were divided into groups with high and low HCC tissue MRP3 expression levels, setting the border to the mean MRP3 expression level in the normal liver tissues, 0.743, the peripheral blood MRP3-specific T cell frequency was significantly higher in the low- than in the high-level group ($p < 0.05$) (Fig. 6B). The CMVpp65-specific T cell frequency was not significantly different between the 2 groups.

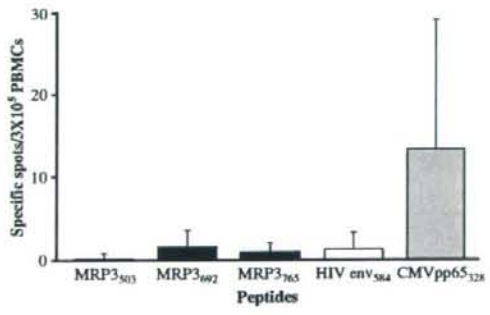

Fig. 3. Direct ex-vivo analysis (IFN-γ ELISPOT assay) of peripheral blood T cell responses to MRP3-derived peptides (peptides $MRP3_{503}$, $MRP3_{692}$, and $MRP3_{765}$: solid bars) or control peptides (peptides $HIVenv_{584}$ and $CMVpp65_{328}$: open and grey bars, respectively) in healthy normal donors. The data are expressed as means + SD.

3.7. Enhancement of MRP3-specific T cell responses after anti-cancer treatment

Several studies including our report have clarified that HCC treatment enhanced HCC-specific immune responses [9,26,27]. We investigated whether MRP3-specific T cell responses observed in HCC patients were enhanced by HCC treatment. In 12 patients who underwent TAE or radiofrequency ablation (RFA) or both

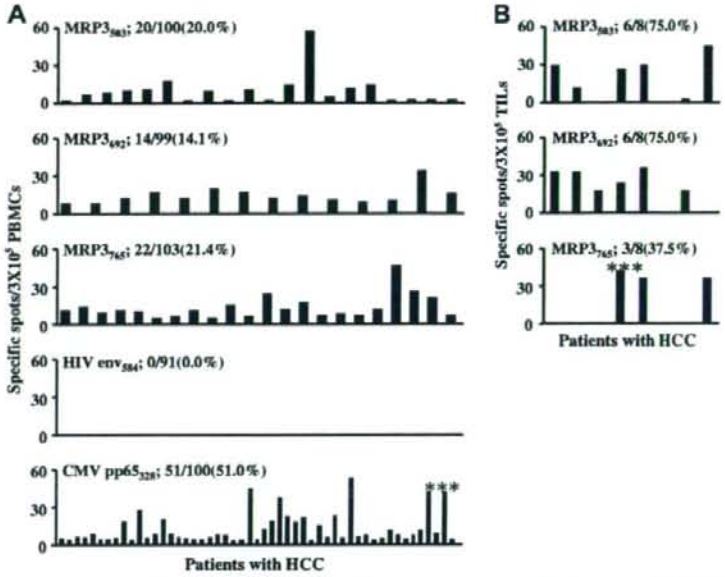

Fig. 4. Direct ex-vivo analysis (IFN-γ ELISPOT assay) of PBMCs (A) and TILs (B) response to MRP3-derived peptides (peptides $MRP3_{503}$, $MRP3_{692}$, and $MRP3_{765}$) or control peptides (peptides $HIVenv_{584}$ and $CMVpp65_{328}$) in HCC patients. Only significant IFN-γ responses are included. Responses to peptides $MRP3_{503}$, $MRP3_{692}$, and $MRP3_{765}$ were considered positive if more than the mean + 3SD specific spots in healthy normal donors were detected and if the number of spots in the presence of antigen was at least twofold greater than that in its absence. Responses to peptides $HIVenv_{584}$ and $CMVpp65_{328}$ were considered positive if more than 10 specific spots were detected and if the number of spots in the presence of antigen was at least twofold greater than that in its absence. The peptide sequences are described in Table 2. * denotes 770 specific spots. ** denotes 210 specific spots. * denotes 72 specific spots.**

without MRP3-specific T-cell responses before treatment, changes in the MRP3-specific T cell frequency were investigated by measuring the frequency by ELISPOT assay before and after treatment. The $MRP3_{503}$, $MRP3_{692}$, or $MRP3_{765}$ peptide-specific T cell frequency was increased after treatment in 8 of the 12 patients (Table 4). In contrast, the immune response to $HIVenv_{584}$ peptide was not enhanced in any patient, and that to $CMVpp65_{328}$ peptide was enhanced in one patient.

4. Discussion

The expression of MRP3 has been reported in several normal tissues and cancer cells [14,15,28,29]. Although MRP3 expression in HCC tissue was confirmed by immunohistochemical staining [16], the expression level varied among patients, and a conclusion has not been reached as to whether the expression is increased compared to that in normal liver tissue [16,17]. In this study, MRP3 expression in HCC tissue was detected in all 20 HCC patients, and the expression level was significantly higher than that in non-cancerous tissue.

The presence of MRP3-recognizing CTL has been reported in lung, colon, bladder, and renal cancer patients [13,30]. However, to our knowledge, there is no report showing the presence of MRP3-specific CTL in HCC patients. In this study, we showed that MRP3-specific CTL could be induced by stimulating PBMCs with MRP3-derived peptides, and the induced CTL showed cytotoxicity against hepatoma cell lines overexpressing MRP3. Based on these findings, we confirmed that MRP3-specific CTLs exist in HCC patients and MRP3 serves as an immunogenic antigen in HCC.

The frequency of peripheral blood CTL specific to each MRP3 epitope was similar to the reported frequencies of CTL against other tumor antigen epitopes [9,10,31–33]. The CTLs were induced even in an early stage of HCC and regardless of HCV infection. In TILs, MRP3-specific CTL were more frequently detected, compared to that in peripheral blood, suggesting that MRP3-specific CTL are not only present in peripheral blood but also infiltrate into the tumor.

The presence and frequency of MRP3-specific CTL were also confirmed using $MRP3_{765}$ tetramer. However, MRP3-specific CTL could not be detected by ELISPOT assay in 6 patients despite a high frequency being

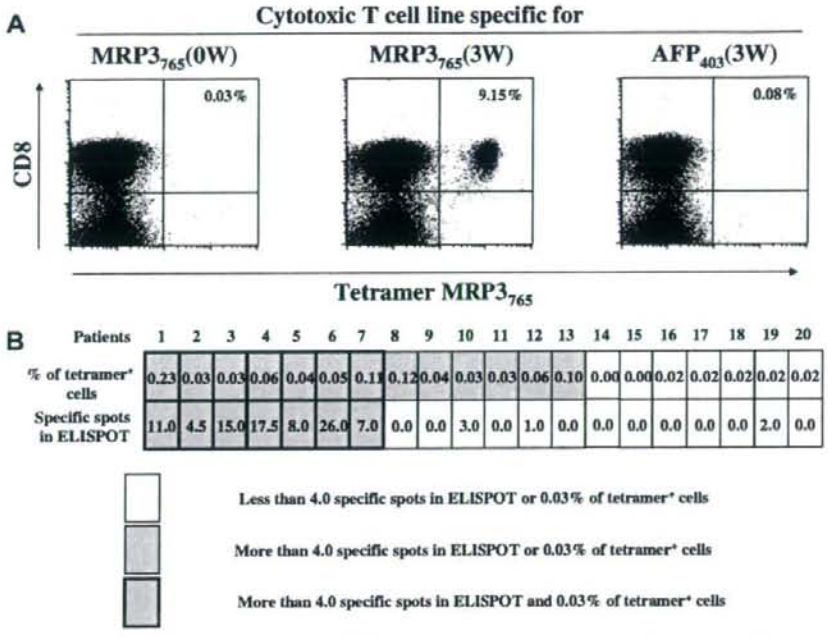

Fig. 5. Detection of MRP3-specific, HLA-A*2402-tetramer$^+$ and CD8$^+$ T lymphocytes in the peripheral blood. (A) Specificity of the $MRP3_{765}$ tetramer was confirmed by staining peptide-specific and non-specific in vitro-expanded T-cell lines. (B) Analysis of the association between the frequency of tetramer$^+$ cells and IFN-γ-producing cells detected on ELISPOT assay was performed in 20 patients.

detected by the tetramer. These findings were similar to those of hTERT-specific CTL in our previous study [10], suggesting the presence of MRP3-specific non-functional T cells in HCC patients.

In the analysis of association between the HCC tissue MRP3 expression level and MRP3-specific T-cell frequency in peripheral blood, a negative correlation was detected, suggesting that MRP3-specific immune responses exert an immune pressure on MRP3-expressing HCC cells. Recent studies have shown the involvement of MRP3 in the resistance to anti-tumor drugs and poor prognosis in several cancer patients [14,15,28,29,34,35]. Taken together with these reports, our results suggest the possibility that MRP3-targeting immunotherapy not only simply eliminates cancers but also improves drug resistance and the prognosis by inhibiting MRP3 expression in cancer cells.

Further to evaluate the usefulness of MRP3 in HCC immunotherapy, we also investigated the association between HCC treatment and the MRP3-specific CTL frequency. As we and other groups previously reported [9,26,27], the MRP3-specific CTL frequency was increased after treatment in 8 of the 12 patients in whom no immune response to MRP3 was detected before treatment, whereas the HIV env_{584}- and $CMVpp65_{328}$-specific CTL frequencies were not increased, excluding one patient, suggesting that this phenomenon represents the enhancement of MRP3-specific immune responses. These findings also confirmed that MRP3 is an antigen expressed in HCC tis-

Table 3
Univariate analysis of the effect of variables on the T cell response against MRP3

	Patients with positive T cell response	Patients without positive T cell response	*p*-value[a]
No. of patients	38	65	
Age (years)[b]	61.4 ± 10.0	64.3 ± 9.7	NS
Sex (M/F)	30/8	49/16	NS
AFP level (≦20/>20)	17/21	21/44	NS
Diff. degree of HCC (well/moderate or poor/ND)	5/14/19	12/21/32	NS
Tumor multiplicity (multiple/solitary)	30/8	43/22	NS
Vascular invasion (+/−)	12/26	18/47	NS
TNM factor			
(T1/T2–4)	6/32	18/47	NS
(N0/N1)	36/2	64/1	NS
(M0/M1)	36/2	57/8	NS
TNM stage (I/II–IV)	6/32	18/47	NS
Histology of non-tumor liver (LC/chronic hepatitis)	30/8	55/10	NS
Liver function (Child A/B/C)	23/14/1	38/25/2	NS
Etiology (HCV/HBV/others)	26/7/5	49/12/4	NS

[a] NS, not significant.
[b] Data are expressed as means ± SD.
[c] ND, not determined.

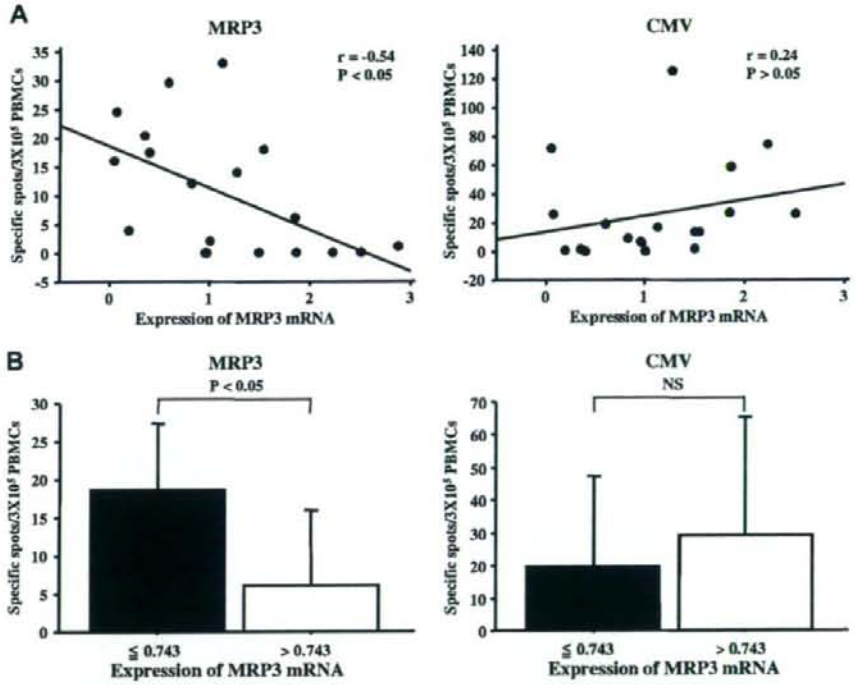

Fig. 6. Analysis of the association between the frequencies of MRP3- specific T cells detected on ELSPOT assay and the expression levels of MRP3 mRNA in HCC tissues. The frequency of MRP3-specific T cells was calculated by the sum of specific spots against $MRP3_{503}$, $MRP3_{692}$, and $MRP3_{765}$ peptides. (A) Linear regression lines for the relationship between the expression of MRP3 mRNA and the frequency of MRP3- or CMVpp65-specific T cells were calculated using Pearson's correlation coefficient. (B) Analysis of the frequency of MRP3- or CMVpp65-specific T cells in patients with low and high expression levels of MRP3 mRNA in HCC tissues.

sue, and has strong immunogenicity that readily induces CTL in vivo.

In conclusion, our study demonstrates that MRP3 is a potential candidate for tumor antigen with strong immunogenicity in HCC immunotherapy.

Acknowledgements

The authors thank Maki Kawamura, Kazumi Fushimi, Nami Nishiyama and Mikiko Nakamura for technical assistance.

Table 4
T cell response to MRP3-derived peptides by ELISPOT assay before and after treatment

	Treatment[a]	Before treatment					After treatment				
		$MRP3_{503}$	$MRP3_{692}$	$MRP3_{765}$	$HIVenv_{584}$	$CMVpp65_{328}$	$MRP3_{503}$	$MRP3_{692}$	$MRP3_{765}$	$HIVenv_{584}$	$CMVpp65_{328}$
Patient 1	TAE + RF	1	0	0	0	9	**5**	5	3	2	6
Patient 2	TAE + RF	0	0	0	0	0	**2**	2	0	0	2
Patient 3	TAE + RF	0	2	0	4	5	**8**	1	**6**	2	**13**
Patient 4	TAE + RF	0	0	0	0	**16**	0	0	0	0	**46**
Patient 5	TAE + RF	0	4	0	1	3	**5**	0	**37**	0	ND[b]
Patient 6	TAE + RF	0	0	0	0	**61**	0	0	4	1	**59**
Patient 7	TAE	0	0	0	0	**92**	0	0	**6**	0	**129**
Patient 8	TAE	0	1	0	1	9	0	1	0	0	0
Patient 9	RF	0	0	0	0	**74**	**6**	7	2.5	2.5	**65**
Patient 10	RF	0	0	0	0.5	0	**3**	0	1	0.5	9.5
Patient 11	RF	1.5	0	1	1	9.5	0	3	**9.5**	1	5.5
Patient 12	RF	0	0	0	0	**13**	0	0	0	0	6

Bold and underlined letters indicate a significant increase as described in materials and methods.

[a] TAE, transcatheter arterial embolization; RF, radiofrequency ablation.

[b] ND: not determined.

References

[1] Llovet JM, Burroughs A, Bruix J. Hepatocellular carcinoma. Lancet 2003;362:1907–1917.

[2] Lin SM, Lin CJ, Lin CC, Hsu CW, Chen YC. Radiofrequency ablation improves prognosis compared with ethanol injection for hepatocellular carcinoma < or =4 cm. Gastroenterology 2004;127:1714–1723.

[3] Ercolani G, Grazi GL, Ravaioli M, Del Gaudio M, Gardini A, Cescon M, et al. Liver resection for hepatocellular carcinoma on cirrhosis: univariate and multivariate analysis of risk factors for intrahepatic recurrence. Ann Surg 2003;237:536–543.

[4] Omata M, Tateishi R, Yoshida H, Shiina S. Treatment of hepatocellular carcinoma by percutaneous tumor ablation methods: ethanol injection therapy and radiofrequency ablation. Gastroenterology 2004;127:S159–S166.

[5] Butterfield LH, Ribas A, Meng WS, Dissette VB, Amarnani S, Vu HT, et al. T-cell responses to HLA-A*0201 immunodominant peptides derived from alpha-fetoprotein in patients with hepatocellular cancer. Clin Cancer Res 2003;9:5902–5908.

[6] Shang XY, Chen HS, Zhang HG, Pang XW, Qiao H, Peng JR, et al. The spontaneous CD8+ T-cell response to HLA-A2-restricted NY-ESO-1b peptide in hepatocellular carcinoma patients. Clin Cancer Res 2004;10:6946–6955.

[7] Zerbini A, Pilli M, Soliani P, Ziegler S, Pelosi G, Orlandini A, et al. Ex vivo characterization of tumor-derived melanoma antigen encoding gene-specific CD8+cells in patients with hepatocellular carcinoma. J Hepatol 2004;40:102–109.

[8] Komori H, Nakatsura T, Senju S, Yoshitake Y, Motomura Y, Ikuta Y, et al. Identification of HLA-A2- or HLA-A24-restricted CTL epitopes possibly useful for glypican-3-specific immunotherapy of hepatocellular carcinoma. Clin Cancer Res 2006;12:2689–2697.

[9] Mizukoshi E, Nakamoto Y, Tsuji H, Yamashita T, Kaneko S. Identification of alpha-fetoprotein-derived peptides recognized by cytotoxic T lymphocytes in HLA-A24+ patients with hepatocellular carcinoma. Int J Cancer 2006;118:1194–1204.

[10] Mizukoshi E, Nakamoto Y, Marukawa Y, Arai K, Yamashita T, Tsuji H, et al. Cytotoxic T cell responses to human telomerase reverse transcriptase in patients with hepatocellular carcinoma. Hepatology 2006;43:1284–1294.

[11] Borst P, Elferink RO. Mammalian ABC transporters in health and disease. Annu Rev Biochem 2002;71:537–592.

[12] Kiuchi Y, Suzuki H, Hirohashi T, Tyson CA, Sugiyama Y. cDNA cloning and inducible expression of human multidrug resistance associated protein 3 (MRP3). FEBS Lett 1998;433:149–152.

[13] Yamada A, Kawano K, Koga M, Matsumoto T, Itoh K. Multidrug resistance-associated protein 3 is a tumor rejection antigen recognized by HLA-A2402-restricted cytotoxic T lymphocytes. Cancer Res 2001;61:6459–6466.

[14] Tada Y, Wada M, Migita T, Nagayama J, Hinoshita E, Mochida Y, et al. Increased expression of multidrug resistance-associated proteins in bladder cancer during clinical course and drug resistance to doxorubicin. Int J Cancer 2002;98:630–635.

[15] Young LC, Campling BG, Cole SP, Deeley RG, Gerlach JH. Multidrug resistance proteins MRP3, MRP1, and MRP2 in lung cancer: correlation of protein levels with drug response and messenger RNA levels. Clin Cancer Res 2001;7:1798–1804.

[16] Nies AT, Konig J, Pfannschmidt M, Klar E, Hofmann WJ, Keppler D. Expression of the multidrug resistance proteins MRP2 and MRP3 in human hepatocellular carcinoma. Int J Cancer 2001;94:492–499.

[17] Zollner G, Wagner M, Fickert P, Silbert D, Fuchsbichler A, Zatloukal K, et al. Hepatobiliary transporter expression in human hepatocellular carcinoma. Liver Int 2005;25:367–379.

[18] Araki T, Itai Y, Furui S, Tasaka A. Dynamic CT densitometry of hepatic tumors. AJR Am J Roentgenol 1980;135:1037–1043.

[19] Liver cancer study group of Japan. General rules for the clinical and pathological study of primary liver cancer. Second English Edition. Kanehara & Co., Ltd., Tokyo. 2003.

[20] Desmet VJ, Gerber M, Hoofnagle JH, Manns M, Scheuer PJ. Classification of chronic hepatitis: diagnosis, grading and staging. Hepatology 1994;19:1513–1520.

[21] Oiso M, Eura M, Katsura F, Takiguchi M, Sobao Y, Masuyama K, et al. A newly identified MAGE-3-derived epitope recognized by HLA-A24-restricted cytotoxic T lymphocytes. Int J Cancer 1999;81:387–394.

[22] Honda M, Yamashita T, Ueda T, Takatori H, Nishino R, Kaneko S. Different signaling pathways in the livers of patients with chronic hepatitis B or chronic hepatitis C. Hepatology 2006;44:1122–1138.

[23] Mizukoshi E, Nascimbeni M, Blaustein JB, Mihalik K, Rice CM, Liang TJ, et al. Molecular and immunological significance of chimpanzee major histocompatibility complex haplotypes for hepatitis C virus immune response and vaccination studies. J Virol 2002;76:6093–6103.

[24] Ikeda-Moore Y, Tomiyama H, Miwa K, Oka S, Iwamoto A, Kaneko Y, et al. Identification and characterization of multiple HLA-A24-restricted HIV-1 CTL epitopes: strong epitopes are derived from V regions of HIV-1. J Immunol 1997;159:6242–6252.

[25] Kuzushima K, Hayashi N, Kimura H, Tsurumi T. Efficient identification of HLA-A*2402-restricted cytomegalovirus-specific CD8(+) T-cell epitopes by a computer algorithm and an enzyme-linked immunospot assay. Blood 2001;98:1872–1881.

[26] Zerbini A, Pilli M, Penna A, Pelosi G, Schianchi C, Molinari A, et al. Radiofrequency thermal ablation of hepatocellular carcinoma liver nodules can activate and enhance tumor-specific T-cell responses. Cancer Res 2006;66:1139–1146.

[27] Ayaru L, Pereira SP, Alisa A, Pathan AA, Williams R, Davidson B, et al. Unmasking of alpha-fetoprotein-specific CD4(+) T cell responses in hepatocellular carcinoma patients undergoing embolization. J Immunol 2007;178:1914–1922.

[28] Konig J, Hartel M, Nies AT, Martignoni ME, Guo J, Buchler MW, et al. Expression and localization of human multidrug resistance protein (ABCC) family members in pancreatic carcinoma. Int J Cancer 2005;115:359–367.

[29] Steinbach D, Wittig S, Cario G, Viehmann S, Mueller A, Gruhn B, et al. The multidrug resistance-associated protein 3 (MRP3) is associated with a poor outcome in childhood ALL and may account for the worse prognosis in male patients and T-cell immunophenotype. Blood 2003;102:4493–4498.

[30] Komohara Y, Harada M, Arima Y, Suekane S, Noguchi M, Yamada A, et al. Anti-cancer vaccine candidates in specific immunotherapy for bladder carcinoma. Int J Oncol 2006;29:1555–1560.

[31] Nagorsen D, Keilholz U, Rivoltini L, Schmittel A, Letsch A, Asemissen AM, et al. Natural T-cell response against MHC class I epitopes of epithelial cell adhesion molecule, her-2/neu, and carcinoembryonic antigen in patients with colorectal cancer. Cancer Res 2000;60:4850–4854.

[32] Griffioen M, Borghi M, Schrier PI, Osanto S. Detection and quantification of CD8(+) T cells specific for HLA-A*0201-binding melanoma and viral peptides by the IFN-gamma-ELISPOT assay. Int J Cancer 2001;93:549–555.

[33] Rentzsch C, Kayser S, Stumm S, Watermann I, Walter S, Stevanovic S, et al. Evaluation of pre-existent immunity in patients with primary breast cancer: molecular and cellular assays to quantify antigen-specific T lymphocytes in peripheral blood mononuclear cells. Clin Cancer Res 2003;9:4376–4386.

[34] Oguri T, Isobe T, Fujitaka K, Ishikawa N, Kohno N. Association between expression of the MRP3 gene and exposure to platinum drugs in lung cancer. Int J Cancer 2001;93:584–589.

[35] Steinbach D, Lengemann J, Voigt A, Hermann J, Zintl F, Sauerbrey A. Response to chemotherapy and expression of the genes encoding the multidrug resistance-associated proteins MRP2, MRP3, MRP4, MRP5, and SMRP in childhood acute myeloid leukemia. Clin Cancer Res 2003;9:1083–1086.

Common Transcriptional Signature of Tumor-Infiltrating Mononuclear Inflammatory Cells and Peripheral Blood Mononuclear Cells in Hepatocellular Carcinoma Patients

Yoshio Sakai, Masao Honda, Haruo Fujinaga, Isamu Tatsumi, Eishiro Mizukoshi, Yasunari Nakamoto, and Shuichi Kaneko

Department of Gastroenterology, Kanazawa University, School of Medicine, Kanazawa, Japan

Abstract

Hepatocellular carcinoma (HCC) is frequently associated with infiltrating mononuclear inflammatory cells. We performed laser capture microdissection of HCC-infiltrating and noncancerous liver-infiltrating mononuclear inflammatory cells in patients with chronic hepatitis C (CH-C) and examined gene expression profiles. HCC-infiltrating mononuclear inflammatory cells had an expression profile distinct from noncancerous liver-infiltrating mononuclear inflammatory cells; they differed with regard to genes involved in biological processes, such as antigen presentation, ubiquitin-proteasomal proteolysis, and responses to hypoxia and oxidative stress. Immunohistochemical analysis and gene expression databases suggested that the up-regulated genes involved macrophages and Th1 and Th2 CD4 cells. We next examined the gene expression profile of peripheral blood mononuclear cells (PBMC) obtained from CH-C patients with or without HCC. The expression profiles of PBMCs from patients with HCC differed significantly from those of patients without HCC ($P < 0.0005$). Many of the up-regulated genes in HCC-infiltrating mononuclear inflammatory cells were also differentially expressed by PBMCs of HCC patients. Analysis of the commonly up-regulated or down-regulated genes in HCC-infiltrating mononuclear inflammatory cells and PBMCs of HCC patients showed networks of nucleophosmin, SMAD3, and proliferating cell nuclear antigen that are involved with redox status, the cell cycle, and the proteasome system, along with immunologic genes, suggesting regulation of anticancer immunity. Thus, exploring the gene expression profile of PBMCs may be a surrogate approach for the assessment of local HCC-infiltrating mononuclear inflammatory cells. [Cancer Res 2008;68(24):10267–79]

Introduction

Hepatocellular carcinoma (HCC) is one of the most frequent malignancies worldwide (1). It commonly develops from chronic liver diseases, such as viral hepatitis (2) and chronic hepatitis, resulting from hepatitis C virus (HCV) infection, is a major risk factor. Indeed, 7% of patients with liver cirrhosis (LC) caused by persistent HCV (LC-C) infection develop HCC annually (3).

Cancer tissues are often associated with infiltrating inflammatory cells, such as tumor-associated macrophages (4), T lymphocytes (5), and antigen-presenting cells (6). These tumor-infiltrating mononuclear inflammatory cells are thought to be important modulators of HCC (7). However, their actual role remains controversial. Increased numbers in HCC have been correlated with a fair prognosis (8), but tumor-infiltrating mononuclear inflammatory cells in HCC tissues have also been found to involve more FOXP3$^+$ regulatory T cells (9) and provide a cancer-favorable environment that leads to resistance to therapy. Characterization of tumor-infiltrating mononuclear inflammatory cells may be valuable in understanding tumor immunology and, possibly, in predicting the prognosis of HCC patients (7).

Peripheral blood mononuclear cells (PBMCs) consist of immune cells, such as monocytes and lymphocytes, and are essential players in the host immune defense system, which responds to various abnormal conditions in the host (10). PBMCs and tumor-infiltrating mononuclear inflammatory cells contain CTLs, specifically cytocidal to cancer tissues (11) and regulatory T cells that can suppress the host immune response against cancer (9). Thus, PBMCs may potentially reflect host immune status. However, there are limited assays for assessing the immune status of PBMCs, such as a proliferation assay, measurements of cytokine production, and the assessment of cytocidal potential.

The advent of cDNA microarray technology for the analysis of gene expression profiles has been useful in comprehensively disclosing underlying molecular features and has provided considerable information for basic science and clinical medicine. We have analyzed gene expression in liver diseases (12, 13) and believe it may become a useful diagnostic tool using liver tissue biopsy samples (14). We have also reported that gene expression profiling of PBMCs predicted the effect of IFN for the eradication of HCV (15) and can provide biomarkers not only for the control of blood sugar but also possibly for predisposing diabetic factors (16). Gene expression profiling of PBMCs from patients with renal cell carcinoma can be used to predict their response to systemic chemotherapy (17). Thus, gene expression information from the cellular components of peripheral blood may be useful in interpreting the internal condition of the patient.

In this study, we used DNA microarray technology to examine differences in gene expression profiles between HCC-infiltrating and noncancerous liver-infiltrating mononuclear inflammatory cells, which were selectively microdissected (12), and the gene expression profiles of PBMCs from LC-C patients with or without HCC. We observed distinct transcriptional features of HCC-infiltrating mononuclear inflammatory cells, reflecting the immune status of the local environment. Intriguingly, the transcriptional features of the HCC-infiltrating mononuclear inflammatory cells were shared with PBMCs from HCC patients. Thus, we suggest the possibility that the gene expression profile of PBMCs may be useful as a clinical surrogate biomarker for the assessment of

Note: Supplementary data for this article are available at Cancer Research Online (http://cancerres.aacrjournals.org/).

Requests for reprints: Shuichi Kaneko, 13-1 Takara-machi, Kanazawa, Ishikawa 920-8641, Japan. Phone: 81-76-265-2233; Fax: 81-76-234-4250; E-mail: skaneko@m-kanazawa.jp.

doi:10.1158/0008-5472.CAN-08-0911

the internal environment of HCC patients with chronic hepatitis C (CH-C) infection.

Materials and Methods

Study subjects. All patients participating in this study had advanced chronic liver disease, cirrhosis, or persistent HCV infection. Twelve patients who developed HCC as a consequence of advanced chronic liver disease related to hepatitis C and who underwent surgical treatment were enrolled (Supplementary Table S1). HCC and noncancerous liver tissues were obtained and frozen. For analysis of gene expression profiles in PBMCs, 32 LC patients without HCC and 30 LC patients with HCC (Supplementary Table S2) were included. Development of HCC was diagnosed by computed tomography (CT) or magnetic resonance imaging with contrast reagents and abdominal angiography with CT imaging in arterial and portal flow phases (18). The pathologic tumor node metastasis classification system of the Liver Cancer Study Group of Japan was used for the staging of HCC. LC was diagnosed by pathologic findings in biopsy specimens where available; otherwise, radiological imaging, platelet counts, serum hyaluronic acid levels, and indocyanine green retention rates were considered for the diagnosis of cirrhosis. The study has been approved by the institutional review board, and informed consent was obtained from all patients enrolled in the study.

Isolation of PBMCs. PBMCs were isolated from heparinized blood samples by Ficoll-Hipaque density gradient centrifugation, as reported previously (15).

Laser capture microdissection. HCC and noncancerous liver tissues obtained during surgery were frozen in optimum cutting temperature compound (Sakura Finetech; ref. 13). All HCC tissues were nodular and clearly separated by noncancerous tissues macroscopically. Cells infiltrating HCC tissues were visualized under a microscope and precisely excised by laser capture microdissection (LCM) using a CRI-337 (Cell Robotics, Inc.), as previously performed (Supplementary Fig. S1*A*; ref. 12). Cells infiltrating noncancerous tissues of CH-C patients were visualized and excised similarly.

RNA isolation and amplification. Total RNA was isolated from PBMCs or tissue samples using a microRNA isolation kit (Stratagene) in accordance with the supplied protocol with slight modifications. Isolated RNA was then amplified twice using antisense RNA and an Amino Allyl MessageAmp aRNA kit (Ambion), as described previously (13). The reference RNA sample was isolated from the PBMCs of a 29-yr-old healthy male volunteer and was amplified in the same manner. Amplified RNAs from the PBMCs of patients and the healthy volunteer were labeled with Cy5 and Cy3 (Amersham), respectively. Equal amounts of amplified RNAs were hybridized to an oligo-DNA chip (AceGene Human Oligo Chip 30K, Hitachi Software Engineering Co., Ltd.) overnight and were then washed for image scanning.

DNA microarray image analysis. The fluorescence intensity of each spot on the oligo-DNA chip was determined using a DNA Microarray Scan Array G (PerkinElmer). The images obtained were quantified using a DNASIS array (v2.6, Hitachi Software Engineering Co., Ltd). For normalization, the intensity of each spot without oligo-DNA was subtracted from that with oligo-DNA in the same block. A validated spot was determined when the intensity of the spot was within the intensity ± 2 SDs for each block. By calibrating the median to base quantity, the intensities of all spots were adjusted for normalization between Cy5 and Cy3.

Quantitative real-time detection PCR. Real-time detection PCR (RTD-PCR) was performed as previously described (15). Briefly, template cDNA was synthesized from 1 μg of total RNA using SuperScript II RT (Invitrogen). Primer pairs for chemokine (C-C motif) receptor 1 (*Ccr1*), histone acetyltransferase 1 (*Hat1*), mitogen-activated protein kinase kinase 1 interacting protein 1 (*Map2k1ip1*), phosphatidylinositol glycan anchor biosynthesis, class B (*PigB*), toll-like receptor 2 (*Tlr2*), superoxide dismutase 2 (*Sod2*), cytokeratin 8 (*Krt8*), *Krt18*, *Krt19*, and glyceraldehydes-3-phosphate dehydrogenase, as an internal control of expression, were purchased from the TaqMan assay reagents library (Applied Biosystems). Synthesized cDNA was mixed with the TaqMan Universal Master Mix (Applied Biosystems), as well as each primer pair and reaction was performed using ABI PRISM 7900HT. Relative expression level of each gene was calculated compared with that of internal control in each sample. Results are expressed as means ± SE.

Flow cytometry analysis. Flow cytometry analysis was performed as described previously (19). Briefly, isolated PBMCs were incubated in PBS supplemented with 2% bovine serum albumin (Sigma-Aldrich JAPAN K.K.) with antihuman CCR1 and CCR2 antibodies labeled with Alexa Fluor 647 (Becton Dickinson Pharmingen). The fluorescence intensity of the cells was measured using a FACSort (Becton Dickinson).

Immunohistochemistry. Surgically obtained HCC and noncancerous liver tissues were fixed with neutral buffered formalin, embedded in paraffin, cut into 4-μm sections, and mounted on microscope slides. The fixed slides were deparaffinized and subjected to heat-induced epitope retrieval 98°C for 40 min. After blocking endogenous peroxidase activity in the tissue specimen using 3% hydrogen peroxide, the slides were incubated with appropriately diluted primary antibodies, antihuman CD4 or anti-human CD14 mouse monoclonal antibodies (Visionbiosystems Novocastra). The reaction was visualized by the REAL EnVision Detection System (DAKO) followed by counterstaining with hematoxylin.

Statistical analysis. Hierarchical clustering and principal component analysis of gene expression was performed using BRB-ArrayTools.[1] Fisher's exact test was used to examine the significance of hierarchical clustering in the dendrogram. A class prediction was performed by three nearest neighbors, incorporating genes that were differentially expressed at the $P = 0.002$ significance level, as assessed by the random variance t test (BRB-ArrayTools). For genes to analyze in a pathway, we used a P value of <0.05 with 2,000 permutations to avoid underestimating the presence of meaningful signaling pathways that were coordinately up-regulated or down-regulated with subtle differences (13). The cross-validated misclassification rate was computed, and at least 2,000 permutations were performed for a valid permutation P value. The univariate t values for comparing the classes were used as weights. Student's t-test was performed for RTD-PCR data, and P values of <0.05 were deemed to be statistically significant. The population of CCR1-positive or CCR2-positive cells in PBMCs by flow cytometry analysis was tested for differences (with $P < 0.05$) by the Mann-Whitney U-test, using SPSS software (SPSS Japan, Inc.).

Analysis of expression data for biological processes and networks. As for genes significantly up-regulated or down-regulated in HCC-infiltrating mononuclear inflammatory cells compared with noncancerous liver-infiltrating mononuclear inflammatory cells or in PBMCs in LC without HCC compared with LC with HCC at $P < 0.05$, we have performed analysis of the biological processes using the MetaCore software suite (GeneGo), as described previously (13). Possible networks were created according to the list of the differentially expressed genes using the MetaCore database, a unique curated database of human protein-protein and protein-DNA interactions, transcription factors, and signaling, metabolic, and bioactive molecules. The P value was calculated as described previously (13).

Gene expression data of major leukocyte types and analysis of DNA microarray expression data. Gene expression data for leukocytes were retrieved through publicly accessible databases.[2] The gene set database GDS1775, which includes gene expression data for major leukocyte types, was obtained and subjected to one-way clustering analysis using BRB-Array Tools with genes that were up-regulated in HCC-infiltrating mononuclear inflammatory cells for the enrolled cases above.

Results

Gene expression in mononuclear inflammatory cells infiltrating into HCC tissue. HCC is frequently associated with infiltrating mononuclear inflammatory cells (20), and various attempts have been made to understand their biological significance

[1] http://linus.nci.nih.gov/BRB-ArrayTools.html
[2] http://www.ncbi.nlm.nih.gov/geo/

(8, 9, 21). We selectively obtained HCC-infiltrating mononuclear inflammatory cells by LCM and compared their gene expression profiles with those of noncancerous liver-infiltrating mononuclear inflammatory cells obtained in the same way (Supplementary Fig. S1A; Supplementary Table S1). The gene expression profiles of HCC-infiltrating mononuclear inflammatory cells showed that 115, 206, and 773 genes were up-regulated and 52, 114, and 750 genes were down-regulated compared with those of noncancerous liver-infiltrating mononuclear inflammatory cells at P levels of <0.005, <0.01, and <0.05, respectively (Geo accession no.[3] GSE 10461; Supplementary Fig. S1B).

Genes at the $P < 0.05$ level were analyzed with regard to their role in biological processes in HCC-infiltrating mononuclear inflammatory cells compared with noncancerous liver-infiltrating mononuclear inflammatory cells using the MetaCore pathway analysis software. The significant processes, in which the up-regulated genes in HCC-infiltrating mononuclear inflammatory cells were involved, included antigen presentation, an immunologically important process in antigen-presenting cells, such as monocyte/macrophages and dendritic cells (Table 1; ref. 22). The genes involved in this process were the genes for the CD1d molecule and C-type lectin domain family 4 for glycolipid antigen recognition (23, 24) and CD86, an accessory molecule indispensable for provoking an immune response (25), suggesting an activated immune reaction in these cells. The up-regulated genes in HCC-infiltrating mononuclear inflammatory cells were also involved in the ubiquitin-proteasomal proteolysis process, with significant genes, such as those encoding ubiquitin-conjugating enzymes and proteasome subunits. This process is required to eradicate unnecessary proteins, which are ubiquitinated, and then degraded in proteasomes (26). Processes related to the steps of gene expression, such as transcription by RNA polymerase II, mRNA processing, and the process of the cell cycle were also represented in the genes up-regulated in HCC-infiltrating mononuclear inflammatory cells, indicating enhanced cellular activity. Genes involved in the process of double-strand breaks, such as topoisomerase II α4 (27), and proliferating cell nuclear antigen (PCNA; ref. 28) genes involved in responses to hypoxia and oxidative stress, such as thioredoxin, peroxiredoxin, and antioxidant protein, were also up-regulated, suggesting that HCC-infiltrating mononuclear inflammatory cells were in an activated inflammatory status and under hypoxic or oxidative stress, presumably caused by the HCC. Thus, the profile of up-regulated genes in HCC-infiltrating mononuclear inflammatory cells suggested an inflammatory status, possibly triggered by antigenic stimulation of HCC tissues.

Fewer processes were identified for the down-regulated genes. One intriguing process identified was that of integrin-mediated cell matrix adhesion, suggesting that HCC-infiltrating mononuclear inflammatory cells may be less adhesive in the local tissues where they were found (Supplementary Table S3).

Subpopulation analysis of HCC-infiltrating mononuclear inflammatory cells using immunohistochemistry and transcriptional analysis. Tumor-infiltrating mononuclear inflammatory cells consist of a mixed cell population, including macrophages, effector T cells, and regulatory T cells, which have been considered to be both cancer-favorable or cancer-unfavorable (8, 21). HCC-infiltrating and noncancerous liver-infiltrating mononuclear inflammatory cells were immunohistochemically evaluated to examine the characteristics of the subpopulations. CD14-positive monocytes/macrophages were prominent in HCC-infiltrating mononuclear inflammatory cells, whereas they were rarely observed in noncancerous liver-infiltrating mononuclear inflammatory cells (Fig. 1A). CD4-positive helper T cells were observed in both HCC tissues and noncancerous liver tissues, although in noncancerous liver tissues, these cells tended to accumulate within the aggregates of mononuclear inflammatory cells, whereas they seemed to be scattered in HCC-infiltrating mononuclear inflammatory cells (Fig. 1A).

Next, we examined the genes that were significantly up-regulated in HCC-infiltrating mononuclear inflammatory cells compared with noncancerous liver-infiltrating mononuclear inflammatory cells, relative to subpopulations of leukocytes, and explored how they may be relevant to leukocyte subpopulations, using the database of the human immune cell transcriptome in the Gene Expression Omnibus[3] (Geo accession no. GDS1775), which covers 26 immune regulatory cells, such as T cells, B cells, natural killer cells, macrophages, dendritic cells, basophils, and eosinophils. Among the 206 extracted, up-regulated genes in HCC-infiltrating mononuclear inflammatory cells (at the $P < 0.01$ level), 97 annotated genes were used for one-way hierarchical clusters (Fig. 1B). Most genes among 97 annotated up-regulated genes in HCC-infiltrating mononuclear inflammatory cells were shown to be expressed with higher magnitude in lipopolysaccharide-stimulated or lipopolysaccharide-unstimulated macrophages than in other types of major leukocytes. The next subpopulations, including the second most number of genes for relatively high magnitude of expression, were Th1 and Th2 CD4 cells under conditions supplemented with interleukin-12 (IL-12) and IL-4, respectively (Geo accession no.[3] GSM90858), secreting Th1 and Th2 cytokine profiles, respectively, suggesting that featured genes expressed in HCC-infiltrating mononuclear inflammatory cells were indicative of CD4 helper T cells, secreting a variety of cytokines.

Thus, this expression analysis showed that, in HCC lesions with tumor antigens, there was an accumulation of antigen-presenting cells, monocyte/macrophages, and CD4 helper T cells, which were in a cytokine-secreting condition, with enhanced cellular biological activities, including ubiquitin-proteasomal proteolysis, presumably under a hypoxic and oxidative stress environment caused by the HCC. The overall inflammatory status represented by HCC-infiltrating mononuclear inflammatory cells was not determined in terms of an anticancer effect, because no obvious shift of CD4 helper T cells to the Th1 or Th2 condition was indicated.

Distinct gene expression profile of PBMCs obtained from patients with cirrhotic liver disease complicated with HCC. The HCC-infiltrating mononuclear inflammatory cells were distinct in terms of expressed genes. The putative biological processes involving these up-regulated genes in tumor-infiltrating mononuclear inflammatory cells suggested a general influence of the HCC on the local environment of the host, represented by stress-response genes. We, thus, examined whether PBMCs in the systemic circulation of the patient might also be influenced by the development of HCC. PBMCs were obtained from 30 patients with LC associated with HCC and from 32 patients with LC not associated with HCC, and the gene expression profiles were compared (Geo accession no.[3] GSE10459).

Unsupervised hierarchical clustering analysis using 17,903 filtered genes, the expression values of which were not missing in >50% of the cases, identified two major clusters of patients, with and without HCC (data not shown). To examine the reproducibility and the reliability of the clustering, we excluded